Available online at www.sciencedirect.com
SCIENCE DIRECT®
International Journal of Solids and Structures 42 (2005) 4115–4153
INTERNATIONAL JOURNAL OF SOLIDS and STRUCTURES
www.elsevier.com/locate/ijsolstr

Transient wave propagation of isotropic plates using a higher-order plate theory

S. Yang, F.G. Yuan *

Department of Mechanical and Aerospace Engineering, North Carolina State University, P.O. Box 7921, Raleigh, NC 27695, United States

Received 23 September 2004; received in revised form 16 December 2004
Available online 2 February 2005

Abstract

Transient wave propagation of isotropic thin plates using a higher-order plate theory is presented in this paper. The aim of this investigation is to assess the applicability of the higher-order plate theory in describing wave behavior of isotropic plates at higher frequencies. Both extensional and flexural waves are considered. A complete discussion of dispersion of isotropic plates is first investigated. All the wave modes and wave behavior for each mode in the low and high-frequency ranges are provided in detail. Using the dispersion relation and integral transforms, exact integral solutions for an isotropic plate subjected to pure impulse load and a number of wave excitations based on the higher-order theory are obtained and asymptotic solutions which highlight the physics of waves are also presented. The axisymmetric three-dimensional analytical solutions of linear wave equations are also presented for comparison. Results show that the higher-order theory can predict the wave behavior closely with exact linear wave solutions at higher frequencies.

Keywords: Transient wave propagation; Higher-order plate theory; Three-dimensional elasticity; Dispersion relation; Green's function; Structural health monitoring

0. Introduction

The theory of stress waves of elastic media shows that in an infinite isotropic elastic solid an arbitrary disturbance is propagated by means of three types of bulk waves (Achenbach, 1984), longitudinal (P) waves,

* Corresponding author. Tel.: +1 919 515 5947; fax: +1 919 515 5934.
E-mail address: yuan@eos.ncsu.edu (F.G. Yuan).

0020-7683/$ - see front matter © 2004 Elsevier Ltd. All rights reserved.
doi:10.1016/j.ijsolstr.2004.12.014

shear vertical (SV), and shear horizontal (SH) waves, each traveling with its own constant velocity. Conventional ultrasonic nondestructive methods based on these waves have been used to inspect flaws with some success (Krautkramer and Krautkramer, 1990; Bray and McBride, 1992). Most inspection techniques, such as conventional ultrasonics or eddy currents, require a transducer to be scanned over each point of the structure which is to be inspected. This is a time-consuming process and cannot inspect in inaccessible areas.

For thin plates, the longitudinal and shear vertical waves experience repeated reflections at the upper and lower surfaces alternately and the resulting disturbance propagation from their mutual interference is guided by the plate surfaces and is directed along the plate. The guided wave can be modeled by imposing surface boundary conditions on the equations of motion and can effectively model the wave behavior. However, this approach introduces dispersion phenomenon, that is, the velocity of propagation of a disturbance along the plate being a function of frequency or, equivalently, wavelength. Consequently, the shape of the signal of a wave packet (a short-time wave train) may vary with the distance and time of propagation. An important feature of guided wave propagation is that there are generally an infinite number of modes, each corresponding to a particular mode of wave propagation. In addition, three types of wave modes, extensional, flexural, and SH waves, can coexist at any given frequency. This is in contrast to bulk waves which exhibit primarily three types of waves. Mode conversion can in general occur at boundaries and at any other discontinuities such as defects, thus multi-mode waves need to be interpreted. Another key characteristic of guided waves is that they can propagate over very long distances because the structure, or waveguide, retains the energy by its surface boundaries and a large region can therefore be interrogated for each transducer position efficiently. Consequently, the use of guided waves in the ultrasonic nondestructive evaluation of structural components such as plate-like structures has received considerable attention over the past two decades (Rose, 1999). More recently, active diagnostic techniques are being used by exciting ultrasonic signals from smart materials mounted or embedded in the structure for detecting localized damage in plate-like structures. The development of diagnostic techniques require the study of complicated wave propagation phenomena and relies strongly on the use of predictive modeling tools to enable the best structural health monitoring strategies to be identified and their sensitivities to be evaluated.

Analyzing waves in structures is often categorized into three methods. They are methods based on three-dimensional elasticity, structural theories, and numerical methods. Three-dimensional elasticity wave solutions are scarce, often with the help of Fourier time and space transforms (e.g., Lih and Mal, 1995). Even they exist, to acquire wave solutions at high frequencies involving many wave modes can be very time consuming. Numerical methods such as finite element and finite difference analyses are particularly very suited to structures of very complex geometry. Due to their approximate nature, dispersion error can incur in the wave propagation solutions. Although it is possible to reduce the dispersion error by simply refining the discretization in space and time, such refinement imposes significant increase in computational cost, especially at high frequencies. In addition, the numerical results are difficult to provide physical interpretation of the wave phenomena. Overall, the computational requirements of the two methods prohibit its use in the majority of practical, real-time structural health monitoring systems. The most popular method is based on structural theories. These theories arrive at comparatively simple but approximate differential equations for describing the wave propagation phenomena. Often the equations can be solved for a wide variety of boundary conditions. One main advantage of the method is due to the efficiency the methods provided without sacrificing much in accuracy. However, the range of applicability can be limited by various constraints (e.g., kinematics) hypotheses with which they are generated.

Most ultrasonic inspection techniques and structural health monitoring applications are based on the generation of fundamental wave modes at low frequencies or with large wavelengths. Usually a single wave mode in a relatively nondispersive low frequency region is excited (Alleyne and Cawley, 1992; Cawley and Alleyne, 1996). Using the low frequency excitations, only a relatively large size of damages can be detected. At higher frequency ranges beyond the cut-off frequencies however, the wavelengths are much smaller which allows for smaller damage sizes to be detected and located. This wave mode used for monitoring

may generate a variety of other modes due to interactions with the discontinuity. In addition, different types of wave modes can be used concurrently apart from the lowest order wave. Different types of wave modes may be sensitive to different types of damages.

In examining waves in isotropic solids, traditionally the method of potentials where the modes can be modeled by each potential has been used in which the displacements are expressed in terms of the potentials. Here a displacement approach for the solutions based on the higher-order plate theory and three-dimensional (3-D) elasticity theory is used, that is, solving the displacement equations of motion directly. This method may be extended in analyzing the composites where the potentials do not exist. The range of validity of the higher-order theory is determined through comparison with the solutions by three-dimensional elasticity.

In this paper, a higher-order plate theory is developed to describe the wave behavior in linearly isotropic thin plates. In the context of wave propagation, thin plates are defined as the plate thickness being several times smaller than a typical wavelength. In Section 1, the higher-order plate theory is formulated with non-dimensional variables. The dispersion curves of extensional and flexural waves and their limits in the lower and high frequencies of various wave modes in plate theory are discussed in detail in Section 2. The Green's functions and the wave solutions for a number of wave excitation under axisymmetric deformation are developed in Sections 3 and 4. The methods of stationary phase and Airy approximation are used to obtain comparatively simple asymptotic solutions for the wave response of the plate for large values of time and long distances from the excitation locations. In Section 5, three-dimensional elasticity wave solutions for symmetric and antisymmetric waves under axisymmetric deformation are also solved. A comparison of dispersive curves between the plate and 3-D elasticity solution are made. A comparison of transient wave responses to seven-peak and pure impulse excitations between the two theories are studied and discussed in Section 6. Finally, conclusions are made regarding the validity of the higher-plate theory in the range of frequencies.

1. Formulation of the higher-order plate theory

In modeling the transient wave propagation of thin plate-like structures using two-dimensional plate theory, rather than three-dimensional elasticity theory, it is possible, in principle, to expand the displacement field of a plate in terms of the thickness coordinate up to any desired degree. To account for the effects of transverse shear deformation and rotary inertia and to improve the accuracy of the extensional wave motion by taking the first-order normal strain and second-order transverse shear strains into consideration, a consistent displacement field may be presented in the following by expanding the terms up to the second-order:

$$\begin{aligned} u_1(\mathbf{x},z,t) &= u(\mathbf{x},t) + z\psi_1(\mathbf{x},t) + z^2\varphi_1(\mathbf{x},t),\\ u_2(\mathbf{x},z,t) &= v(\mathbf{x},t) + z\psi_2(\mathbf{x},t) + z^2\varphi_2(\mathbf{x},t),\\ u_3(\mathbf{x},z,t) &= w(\mathbf{x},t) + z\psi_3(\mathbf{x},t), \end{aligned} \tag{1.1}$$

where $\mathbf{x} = (x_1, x_2)$. The x_1–x_2 plane is chosen to lie along the mid-plane of the plate. The generalized displacements $(u, v, w, \psi_1, \psi_2)$ have the same physical meaning as in the first-order shear deformation theory (Reissner, 1945, 1947; Mindlin, 1951), and three additional linear and quadratic terms of z associated with ψ_3, φ_1, and φ_2 are added to the expansion of the displacement field. Note that the displacement field in Eq. (1.1) suggests that the transverse normal to the mid-plane will induce elongation or contraction (Kane and Mindlin, 1956; Mindlin and Medick, 1959; Whitney and Sun, 1973). The linear strains associated with the displacement field Eq. (1.1) are

$$\begin{aligned} &\varepsilon_{11} = \varepsilon_{11}^{(0)} + z\varepsilon_{11}^{(1)} + z^2\varepsilon_{11}^{(2)}, \quad \varepsilon_{22} = \cdots, \quad \gamma_{12} = \cdots,\\ &\varepsilon_{33} = \varepsilon_{33}^{(0)}, \quad \gamma_{23} = \gamma_{23}^{(0)} + z\gamma_{23}^{(1)}, \quad \gamma_{13} = \gamma_{13}^{(0)} + z\gamma_{13}^{(1)}, \end{aligned} \tag{1.2}$$

where

$$\begin{aligned}
&\varepsilon_{11}^{(0)} = u_{,1}, \quad \varepsilon_{11}^{(1)} = \psi_{1,1}, \quad \varepsilon_{11}^{(2)} = \varphi_{1,1}, \quad \ldots,\\
&\varepsilon_{33}^{(0)} = \psi_3,\\
&\gamma_{13}^{(0)} = \psi_1 + w_{,1}, \quad \gamma_{13}^{(1)} = 2\varphi_1 + \psi_{3,1},\\
&\gamma_{23}^{(0)} = \psi_2 + w_{,2}, \quad \gamma_{23}^{(1)} = 2\varphi_2 + \psi_{3,2}.
\end{aligned}$$

However, the discrepancies between the actual displacement field and that of the approximate plate theory need to be corrected by making the following substitutions related to the thickness strains

$$\begin{aligned}
&\kappa_3\varepsilon_{33}^{(0)} \text{ for } \varepsilon_{33}^{(0)},\\
&\kappa_1\gamma_{13}^{(0)} \text{ for } \gamma_{13}^{(0)}, \quad \kappa_4\gamma_{13}^{(1)} \text{ for } \gamma_{13}^{(1)},\\
&\kappa_2\gamma_{23}^{(0)} \text{ for } \gamma_{23}^{(0)}, \quad \kappa_5\gamma_{23}^{(1)} \text{ for } \gamma_{23}^{(1)},
\end{aligned} \tag{1.3}$$

where κ_i ($i = 1$–5) are the corrected coefficients similar to those introduced by Mindlin and Medick (1959). Matching the cut-off frequencies of the following modes: (1) plate extensional modes and the first two symmetric modes of 3-D elasticity theory; (2) plate flexural mode with the second antisymmetric mode of 3-D elasticity theory, the corrected coefficients are chosen as $\kappa_1 = \kappa_2 = \kappa = \sqrt{\pi^2/12}$, $\kappa_3 = \kappa$, $\kappa_4 = \kappa_5 = \sqrt{\pi^2/15}$ (Whitney and Sun, 1973).

The constitutive equations for a linear elastic plate may be derived from the strain energy density in the 3-D elasticity theory with the corrections made by Eq. (1.3). For isotropic material the plate constitutive equations are

$$\begin{Bmatrix} N_{11} \\ N_{22} \\ N_{12} \end{Bmatrix} = \begin{bmatrix} \lambda+2G & \lambda & 0 \\ \lambda & \lambda+2G & 0 \\ 0 & 0 & G \end{bmatrix} \left(h \begin{Bmatrix} u_{,1} \\ v_{,2} \\ u_{,2}+v_{,1} \end{Bmatrix} + \frac{h^3}{12} \begin{Bmatrix} \varphi_{1,1} \\ \varphi_{2,2} \\ \varphi_{1,2}+\varphi_{2,1} \end{Bmatrix} \right) + h\kappa\lambda \begin{Bmatrix} 1 \\ 1 \\ 0 \end{Bmatrix} \psi_3, \tag{1.3a}$$

$$N_{33} = h\left[\kappa\lambda(u_{,1}+v_{,2}) + \kappa^2(\lambda+2G)\psi_3\right] + \frac{h^3}{12}\kappa\lambda(\varphi_{1,1}+\varphi_{2,2}), \tag{1.3b}$$

$$\begin{Bmatrix} R_2 \\ R_1 \end{Bmatrix} = \kappa_4^2 \frac{h^3}{12} G \begin{Bmatrix} 2\varphi_2 + \psi_{3,2} \\ 2\varphi_1 + \psi_{3,1} \end{Bmatrix}, \tag{1.3c}$$

$$\begin{Bmatrix} S_{11} \\ S_{22} \\ S_{12} \end{Bmatrix} = \begin{bmatrix} \lambda+2G & \lambda & 0 \\ \lambda & \lambda+2G & 0 \\ 0 & 0 & G \end{bmatrix} \left(\frac{h^3}{12} \begin{Bmatrix} u_{,1} \\ v_{,2} \\ u_{,2}+v_{,1} \end{Bmatrix} + \frac{h^5}{80} \begin{Bmatrix} \varphi_{1,1} \\ \varphi_{2,2} \\ \varphi_{1,2}+\varphi_{2,1} \end{Bmatrix} \right) + \kappa\frac{h^3}{12}\lambda \begin{Bmatrix} 1 \\ 1 \\ 0 \end{Bmatrix} \psi_3, \tag{1.3d}$$

$$\begin{Bmatrix} M_{11} \\ M_{22} \\ M_{12} \end{Bmatrix} = \frac{h^3}{12} \begin{bmatrix} \lambda+2G & \lambda & 0 \\ \lambda & \lambda+2G & 0 \\ 0 & 0 & G \end{bmatrix} \begin{Bmatrix} \psi_{1,1} \\ \psi_{2,2} \\ \psi_{1,2}+\psi_{2,1} \end{Bmatrix}, \tag{1.3e}$$

$$\begin{Bmatrix} Q_2 \\ Q_1 \end{Bmatrix} = \kappa^2 hG \begin{Bmatrix} w_{,2}+\psi_2 \\ w_{,1}+\psi_1 \end{Bmatrix}, \tag{1.3f}$$

where h is the thickness of the plate, λ and G are the Lame's constants of elasticity, and the stress resultants are defined by

$$\left\{\begin{array}{c} N_{\alpha\beta} \\ M_{\alpha\beta} \\ S_{\alpha\beta} \end{array}\right\} = \int_{-h/2}^{h/2} \sigma_{\alpha\beta} \left\{\begin{array}{c} 1 \\ z \\ z^2/2 \end{array}\right\} \mathrm{d}z, \qquad \left\{\begin{array}{c} Q_\alpha \\ R_\alpha \end{array}\right\} = \int_{-h/2}^{h/2} \sigma_{\alpha 3} \left\{\begin{array}{c} 1 \\ z \end{array}\right\} \mathrm{d}z, \qquad N_3 = \int_{-h/2}^{h/2} \sigma_{33}\, \mathrm{d}z.$$

With the linear strain–displacement relation, the equations of motion of the higher-order plate theory can be derived using the principle of virtual displacements or Hamilton's principle (e.g., Washizu, 1982)

$$0 = \int_{t_1}^{t_2} (\delta U + \delta V - \delta K)\, \mathrm{d}t, \tag{1.4}$$

where δU is the virtual strain energy, δV virtual work done by applied forces, and δK the virtual kinetic energy. For an isotropic plate with mid-plane parallel to the plane $z = 0$, a set of equations of motion is

$$\begin{aligned} &N_{11,1} + N_{12,2} + q_1 = I_0 \ddot{u} + I_2 \ddot{\varphi}_1, \\ &N_{12,1} + N_{22,2} + q_2 = I_0 \ddot{v} + I_2 \ddot{\varphi}_2, \\ &R_{1,1} + N_{2,2} - N_3 + m = I_2 \ddot{\psi}_3, \\ &S_{11,1} + S_{12,2} - R_1 + n_1 = \frac{I_2}{2} \ddot{u} + \frac{I_4}{2} \ddot{\varphi}_1, \\ &S_{12,1} + S_{22,2} - R_2 + n_2 = \frac{I_2}{2} \ddot{v} + \frac{I_4}{2} \ddot{\varphi}_2, \end{aligned} \tag{1.5}$$

$$\begin{aligned} &Q_{1,1} + Q_{2,2} + q = I_0 \ddot{w}, \\ &M_{11,1} + M_{12,2} - Q_1 + m_1 = I_2 \ddot{\psi}_1, \\ &M_{12,1} + M_{22,2} - Q_2 + m_2 = I_2 \ddot{\psi}_2, \end{aligned} \tag{1.6}$$

with a number of boundary conditions which must be specified on the plate edges; $q_1, q_2, \ldots, m_1$ and m_2 are the loads related to the surface tractions and defined by

$$\left\{\begin{array}{c} q_\alpha \\ n_\alpha \end{array}\right\} = [\sigma_{\alpha 3}(h/2) - \sigma_{\alpha 3}(-h/2)] \left\{\begin{array}{c} 1 \\ h^2/4 \end{array}\right\}, \qquad m_\alpha = [\sigma_{\alpha 3}(h/2) + \sigma_{\alpha 3}(-h/2)] \frac{h}{2},$$

$$q = \sigma_{33}(h/2) - \sigma_{33}(-h/2), \qquad m = [\sigma_{33}(h/2) + \sigma_{33}(-h/2)] \frac{h}{2},$$

$$I_j = \int_{-h/2}^{h/2} \rho(z)^j \, \mathrm{d}z \quad (j = 0, 2, 4),$$

here $\alpha = 1, 2$ and ρ is the mass density.

The equations of motion in Eqs. (1.5) and (1.6) can be expressed in terms of generalized displacements by substituting for the stress resultants from the constitutive equations, Eq. (1.3). The equations of motion and the plate constitutive equations indicate that the extensional or symmetric waves with five degrees of freedom $(u, v, \psi_3, \varphi_1, \varphi_2)$ are decoupled from the flexural or antisymmetric waves with three degrees of freedom (w, ψ_1, ψ_2). The symmetric and antisymmetric waves refer to the wave displacement profile symmetric and antisymmetric with respect to the mid-plane of the plate $(z = 0)$ respectively. In the following these two wave motions are examined separately. For isotropic plates, the equations of motion take the form:

Extensional wave

$$\frac{I_0}{\rho}\left[(\lambda+2G)u_{,11}+(\lambda+G)v_{,12}+Gu_{,22}\right]+\frac{I_2}{\rho}\left[(\lambda+2G)\varphi_{1,11}+(\lambda+G)\varphi_{2,12}+G\varphi_{1,22}\right]$$
$$+\kappa\frac{I_0}{\rho}\lambda\psi_{3,1}+q_1=I_0\ddot{u}+I_2\ddot{\varphi}_1 \tag{1.7a}$$

$$\frac{I_0}{\rho}\left[Gv_{,11}+(\lambda+G)u_{,21}+(\lambda+2G)v_{,22}\right]+\frac{I_2}{\rho}\left[G\varphi_{2,11}+(\lambda+G)\varphi_{1,12}+(\lambda+2G)\varphi_{2,22}\right]$$
$$+\kappa\frac{I_0}{\rho}\lambda\psi_{3,2}+q_2=I_0\ddot{v}+I_2\ddot{\varphi}_2, \tag{1.7b}$$

$$\frac{I_2}{\rho}\left[\kappa_4^2G(\psi_{3,11}+\psi_{3,22})+(2\kappa_4^2G-\kappa\lambda)(\varphi_{1,1}+\varphi_{2,2})\right]-\frac{I_0}{\rho}\kappa[\lambda(u_{,1}+v_{,2})+\kappa(\lambda+2G)\psi_3]+m=I_2\ddot{\psi}_3, \tag{1.7c}$$

$$\frac{I_2}{2\rho}\left[(\lambda+2G)u_{,11}+(\lambda+G)v_{,12}+Gu_{,22}+(\kappa\lambda-2\kappa_4^2G)\psi_{3,1}-4\kappa_4^2G\varphi_1\right]$$
$$+\frac{I_4}{2\rho}\left[(\lambda+2G)\varphi_{1,11}+(\lambda+G)\varphi_{2,12}+G\varphi_{1,22}\right]+n_1=\frac{I_2}{2}\ddot{u}+\frac{I_4}{2}\ddot{\varphi}_1, \tag{1.7d}$$

$$\frac{I_2}{2\rho}\left[Gv_{,11}+(\lambda+G)u_{,12}+(\lambda+2G)v_{,22}+(\kappa\lambda-2\kappa_4^2G)\psi_{3,2}-4\kappa_4^2G\varphi_2\right]$$
$$+\frac{I_4}{2\rho}\left[G\varphi_{2,11}+(\lambda+G)\varphi_{1,12}+(\lambda+2G)\varphi_{2,22}\right]+n_2=\frac{I_2}{2}\ddot{v}+\frac{I_4}{2}\ddot{\varphi}_2. \tag{1.7e}$$

Flexural wave

$$\frac{I_0}{\rho}\kappa^2G(w_{,11}+w_{,22}+\psi_{1,1}+\psi_{2,2})+q=I_0\ddot{w}, \tag{1.8a}$$

$$\frac{I_2}{\rho}\left[(\lambda+2G)\psi_{1,11}+(\lambda+G)\psi_{2,12}+G\psi_{1,22}\right]-\frac{I_0}{\rho}\kappa^2G(w_{,1}+\psi_1)+m_1=I_2\ddot{\psi}_1, \tag{1.8b}$$

$$\frac{I_2}{\rho}\left[G\psi_{2,11}+(\lambda+G)\psi_{1,12}+(\lambda+2G)\psi_{2,22}\right]-\frac{I_0}{\rho}\kappa^2G(w_{,2}+\psi_2)+m_2=I_2\ddot{\psi}_2. \tag{1.8c}$$

In the following analysis it is convenient to make the variables dimensionless. To accomplish this step, we may introduce a representative length scale $h/2$, a typical time scale, $\tau=0.5h/c_{\mathrm{T}}$ ($c_{\mathrm{T}}=\sqrt{G/\rho}$ is the velocity of bulk transverse or shear vertical waves), and define the following nondimensional variables and quantities

$$\begin{aligned}
&x_i'=\frac{x_i}{h/2},\quad t'=\frac{t}{\tau},\quad w'=\frac{w}{h/2},\\
&u'=\frac{u}{h/2},\quad v'=\frac{v}{h/2},\quad \varphi_\alpha'=\varphi_\alpha h/2,\\
&q_\alpha'=\frac{q_\alpha}{2G},\quad n_\alpha'=\frac{n_\alpha}{Gh^2/20},\quad m'=\frac{m}{Gh/3},\\
&q'=\frac{q}{2G},\quad m_\alpha'=\frac{m_\alpha}{Gh/3},\\
&k_j'=k_jh/2,\quad \omega'=\omega\tau,
\end{aligned} \tag{1.9}$$

where k'_j, ω' are the nondimensional wave number and frequency which will be used in the dispersion relation. According to the nondimensionalization, the phase velocity and group velocity are normalized by $c_T = \sqrt{G/\rho}$.

In the sequel the bulk longitudinal wave velocity $c_L = \sqrt{(\lambda + 2G)/\rho}$, plate velocity $c_P = \sqrt{E/[(1-\nu^2)\rho]}$ (Graff, 1991), and c_R (Rayleigh wave velocity) are often used and their dimensionless representations normalized by c_T are

$$c'_L = \sqrt{\alpha}, \quad c'_P = 2\sqrt{\frac{\alpha-1}{\alpha}} = \sqrt{\frac{2}{1-\nu}}, \quad c'_R = \frac{c_R}{c_T}, \quad c'_T = 1,$$

where $\alpha = (c_L/c_T)^2 = 2 + \lambda/G = 2(1-\nu)/(1-2\nu)$ and ν is Poisson's ratio. Note that the nondimensional quantities will be used in the following wave analysis and all the "primes" will be dropped except stated otherwise. Then the dimensionless equations of motion can be expressed as

Extensional wave

$$\alpha u_{,11} + (\alpha-1)v_{,12} + u_{,22} + [\alpha\varphi_{1,11} + (\alpha-1)\varphi_{2,12} + \varphi_{1,22}]/3 + \kappa(\alpha-2)\psi_{3,1} + q_1 = \ddot{u} + \ddot{\varphi}_1/3, \tag{1.10a}$$

$$v_{,11} + (\alpha-1)u_{,12} + \alpha v_{,22} + [\varphi_{2,11} + (\alpha-1)\varphi_{1,12} + \alpha\varphi_{2,22}]/3 + \kappa(\alpha-2)\psi_{3,2} + q_2 = \ddot{v} + \ddot{\varphi}_2/3, \tag{1.10b}$$

$$\kappa_4^2(\psi_{3,11} + \psi_{3,22}) - [\kappa(\alpha-2) - 2\kappa_4^2](\varphi_{1,1} + \varphi_{2,2}) - 3\kappa(\alpha-2)(u_{,1} + v_{,2}) - 3\kappa^2\alpha\psi_3 + m = \ddot{\psi}_3, \tag{1.10c}$$

$$\left\{\alpha u_{,11} + (\alpha-1)v_{,12} + u_{,22} + [\kappa(\alpha-2) - 2\kappa_4^2]\psi_{3,1} - 4\kappa_4^2\varphi_1\right\}\frac{5}{3} + \alpha\varphi_{1,11} + (\alpha-1)\varphi_{2,12} + \varphi_{1,22} + n_1 = \frac{5}{3}\ddot{u} + \ddot{\varphi}_1, \tag{1.10d}$$

$$\left\{v_{,11} + (\alpha-1)u_{,12} + \alpha v_{,22} + [\kappa(\alpha-2) - 2\kappa_4^2]\psi_{3,2} - 4\kappa_4^2\varphi_2\right\}\frac{5}{3} + \varphi_{2,11} + (\alpha-1)\varphi_{1,12} + \alpha\varphi_{2,22} + n_2 = \frac{5}{3}\ddot{v} + \ddot{\varphi}_2. \tag{1.10e}$$

Flexural wave

$$\kappa^2(w_{,11} + w_{,22} + \psi_{1,1} + \psi_{2,2}) + q = \ddot{w}, \tag{1.11a}$$

$$\alpha\psi_{1,11} + (\alpha-1)\psi_{2,12} + \psi_{1,22} - 3\kappa^2(w_{,1} + \psi_1) + m_1 = \ddot{\psi}_1, \tag{1.11b}$$

$$\psi_{2,11} + (\alpha-1)\psi_{1,12} + \alpha\psi_{2,22} - 3\kappa^2(w_{,2} + \psi_2) + m_2 = \ddot{\psi}_2. \tag{1.11c}$$

The dimensionless equations depend only on a single parameter α except loading parameters, and thus the dispersion relation discussed below depends solely on the single parameter or Poisson's ratio. This is one advantage of this nondimensionalization.

2. Dimensionless dispersion relation

2.1. Extensional wave

To obtain dispersion relation we set all mechanical loads to zero and seek the plane wave elementary solutions to Eq. (1.10) of the form

$$\mathbf{U} = \boldsymbol{a}\exp[\mathrm{i}(\boldsymbol{k}\cdot\boldsymbol{x} - \omega t)], \tag{2.1}$$

where $\mathbf{U} = [u, v, \psi_3, \varphi_1, \varphi_2]^{\mathrm{T}}$, $\boldsymbol{k} = [k_1, k_2]^{\mathrm{T}}$ is the wave vector, ω is the frequency, and $\boldsymbol{a}$ is the complex-valued vector (or wave amplitude). Substituting Eq. (2.1) into Eq. (1.10), we have the following generalized eigenvalue problem

$$(\boldsymbol{K} - \omega^2 \boldsymbol{M})\boldsymbol{a} = \boldsymbol{0}, \tag{2.2}$$

where $\boldsymbol{K}$ and $\boldsymbol{M}$ are 5×5 matrices expressed by

$$\boldsymbol{K} = \begin{bmatrix} \alpha k_1^2 + k_2^2 & (\alpha-1)k_1k_2 & -\mathrm{i}\kappa(\alpha-2)k_1 & (\alpha k_1^2 + k_2^2)/3 & (\alpha-1)k_1k_2/3 \\ (\alpha-1)k_1k_2 & k_1^2 + \alpha k_2^2 & -\mathrm{i}\kappa(\alpha-2)k_2 & (\alpha-1)k_1k_2/3 & (k_1^2 + \alpha k_2^2)/3 \\ 3\mathrm{i}\kappa(\alpha-2)k_1 & 3\mathrm{i}\kappa(\alpha-2)k_2 & \kappa_4^2(k_1^2+k_2^2) + 3\alpha\kappa^2 & \mathrm{i}[\kappa(\alpha-2) - 2\kappa_4^2]k_1 & \mathrm{i}[\kappa(\alpha-2) - 2\kappa_4^2]k_2 \\ \frac{5}{3}(\alpha k_1^2 + k_2^2) & \frac{5}{3}(\alpha-1)k_1k_2 & -\frac{5}{3}\mathrm{i}[\kappa(\alpha-2) - 2\kappa_4^2]k_1 & \alpha k_1^2 + k_2^2 + \frac{20}{3}\kappa_4^2 & (\alpha-1)k_1k_2 \\ \frac{5}{3}(\alpha-1)k_1k_2 & \frac{5}{3}(k_1^2 + \alpha k_2^2) & -\frac{5}{3}\mathrm{i}[\kappa(\alpha-2) - 2\kappa_4^2]k_2 & (\alpha-1)k_1k_2 & k_1^2 + \alpha k_2^2 + \frac{20}{3}\kappa_4^2 \end{bmatrix},$$

$$\boldsymbol{M} = \begin{bmatrix} 1 & 0 & 0 & 1/3 & 0 \\ 0 & 1 & 0 & 0 & 1/3 \\ 0 & 0 & 1 & 0 & 0 \\ 5/3 & 0 & 0 & 1 & 0 \\ 0 & 5/3 & 0 & 0 & 1 \end{bmatrix}.$$

Setting the determinant of the coefficient matrix in Eq. (2.2) to zero for nontrivial solutions of $\boldsymbol{a}$, $\boldsymbol{k}$ and ω have to be related by

$$|\boldsymbol{K} - \omega^2 \boldsymbol{M}| = 0. \tag{2.3}$$

The eigenrelation Eq. (2.3) describes extensional dispersion relation of the isotropic plate. For a given k, the relation provides five positive eigenvalues ω^2 or ten real solutions for the frequency ω by numerical calculation. When k varies continuously, each pair of the solution represents a wave propagation mode. In fact, the matrices $\boldsymbol{K}$ and $\boldsymbol{M}$ can be expressed as a Hermitian matrix and a real symmetric matrix, respectively, by rewriting Eq. (1.10). The five pairs of real distinct propagation modes may be written as

$$\omega = \pm W_j(\boldsymbol{k}), \quad W_j > 0 \ \ (j = 1, 2, \ldots, 5).$$

For a wave mode, $\omega = W(\boldsymbol{k})$, the phase velocity $\mathbf{c}$ is given by

$$\mathbf{c} = \frac{W}{k}\hat{\mathbf{k}} = c\hat{\mathbf{k}},$$

where $\hat{\mathbf{k}}$ is the unit vector in the $\mathbf{k}$ direction, and the group velocity C_j is given by

$$C_j = \frac{\partial W}{\partial k_j},$$

$\mathbf{k}$ can be expressed using the polar coordinates (k, ϕ) as

$$k_1 = k\cos\phi, \quad k_2 = k\sin\phi, \quad k = |\boldsymbol{k}|,$$

where ϕ is the direction of wave vector $\mathbf{k}$ (or direction of wave propagation) and k is the magnitude of $\mathbf{k}$. In general, $\omega = W(k, \phi)$.

For isotropic plates ω is independent of ϕ. The group velocity $\mathbf{C}$ has a component $\partial W/\partial k$ in the direction of $\mathbf{k}$ and a component $\partial W/k\,\partial\phi = 0$ perpendicular to $\mathbf{k}$. Therefore, the group velocity $\mathbf{C}$ is parallel to $\mathbf{k}$, or $\mathbf{c}$, and

$$\mathbf{C} = C\hat{\mathbf{k}}, \quad C = \frac{\partial W}{\partial k}.$$

Knowing the above fact, expanding the determinant in Eq. (2.3) leads to following wave modes:

$$\omega^2 = k^2, \tag{2.4}$$

$$\omega^2 = k^2 + \pi^2, \tag{2.5}$$

$$\begin{vmatrix} \alpha k^2 - \omega^2 & (\alpha k^2 - \omega^2)/3 & -\mathrm{i}\kappa(\alpha-2)k \\ \frac{5}{3}(\alpha k^2 - \omega^2) & \alpha k^2 + \frac{20}{3}\kappa_4^2 - \omega^2 & -\frac{5}{3}\mathrm{i}[\kappa(\alpha-2) - 2\kappa_4^2]k \\ 3\mathrm{i}\kappa(\alpha-2)k & \mathrm{i}[\kappa(\alpha-2) - 2\kappa_4^2]k & \kappa_4^2 k^2 + 3\alpha\kappa^2 - \omega^2 \end{vmatrix} = 0$$

or

$$\begin{vmatrix} \alpha k^2 - \omega^2 & (\alpha k^2 - \omega^2)/3 & \kappa(\alpha-2)k \\ \frac{5}{3}(\alpha k^2 - \omega^2) & \alpha k^2 + \frac{20}{3}\kappa_4^2 - \omega^2 & \frac{5}{3}[\kappa(\alpha-2) - 2\kappa_4^2]k \\ 3\kappa(\alpha-2)k & [\kappa(\alpha-2) - 2\kappa_4^2]k & \kappa_4^2 k^2 + 3\alpha\kappa^2 - \omega^2 \end{vmatrix} = 0. \tag{2.6}$$

Eq. (2.6) can be written in a polynomial form as

$$\omega^6 + \alpha_1\omega^4 + \alpha_2\omega^2 + \alpha_3 = 0, \tag{2.7}$$

with

$$\begin{aligned} \alpha_1 &= -(2\alpha + \kappa_4^2)k^2 - 3(\alpha\kappa^2 + 5\kappa_4^2), \\ \alpha_2 &= \alpha(\alpha + 2\kappa_4^2)k^4 + 3[(\alpha^2 + 4\alpha - 4)\kappa^2 + 5\alpha\kappa_4^2]k^2 + 45\alpha\kappa^2\kappa_4^2, \\ \alpha_3 &= -[\alpha^2\kappa_4^2 k^4 + 12\kappa^2(\alpha-1)(\alpha k^2 + 15\kappa_4^2)]k^2. \end{aligned} \tag{2.8}$$

Fig. 1(a) shows the group velocity C as a function of frequency ω for each extensional wave mode for an isotropic plate with $v = 0.33$. The five modes are labeled as T_0, T_1, T_2, T_3, and T_4. The modes T_3 and T_4 represent the SH waves. The corresponding wave displacements do not have the transverse component w and are perpendicular to the wave propagation direction. Because the displacements for the modes are symmetric with respect to $z = 0$, they may be called symmetric SH waves.

In the following, each pair of wave mode shown in Eqs. (2.4)–(2.6) is described separately, mainly focusing on their velocity limits in the low and high frequency ranges.

Wave mode T_3: $\omega^2 = k^2$

The wave mode T_3 shown in Fig. 1 and is represented by Eq. (2.4). The mode is not dispersive, and the phase and group velocities are:

$$c = C = c_{\mathrm{T}}.$$

Clearly this mode is shear waves. The eigenvector $\boldsymbol{a}$ corresponding to the mode, $\omega^2 = k^2$, shows that the displacement perpendicular to $\mathbf{k}$, $u_\theta = v\cos\phi - u\sin\phi$ is the only nonzero component in the circumferential direction, thus SH waves. For example, let $\boldsymbol{k} = [k_1, 0]^{\mathrm{T}}$, the displacement vector $[u, v, w]$ for the mode is in the x_2 direction.

Wave mode T_4: $\omega^2 = k^2 + \pi^2$

$$c = \frac{\sqrt{k^2 + \pi^2}}{k} = \frac{\omega}{\sqrt{\omega^2 - \pi^2}}, \quad C = \frac{1}{c}.$$

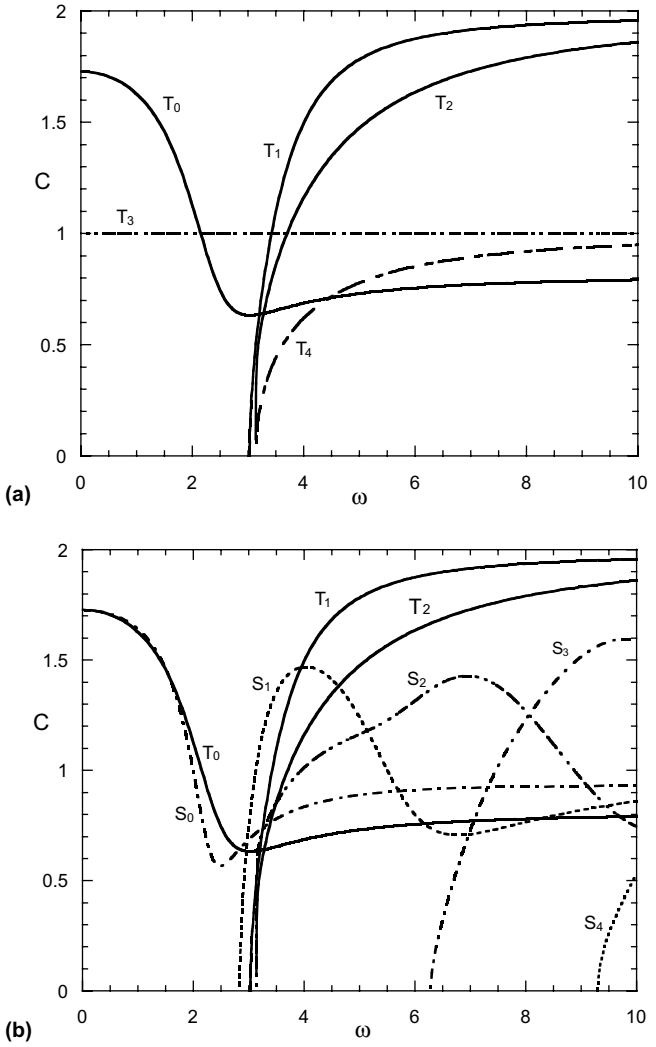

Fig. 1. Group velocity dispersion relation of extensional waves ($v = 0.33$): (a) five modes based on plate theory, (b) axisymmetric wave modes of plate theory and 3-D elasticity.

This SH mode possesses the following cut-off frequency ω_c which can be determined by setting $k \to 0$,

$$\omega_c = \sqrt{15}\kappa_4 = \pi,$$

and the wave speeds approach the pure shear waves as $k \to \infty$

$$c, C \sim c_{\mathrm{T}} \quad \text{as } k \to \infty.$$

For the symmetric SH waves in a plate, the 3-D elasticity provides the following dispersion relation explicitly

$$\omega^2 = k^2 + \left(\frac{n\pi}{2}\right)^2, \quad n = 0, 2, 4, \ldots$$

Hence, the modes T_3 and T_4 coincide with the first two of SH wave modes in 3-D elasticity.

Wave modes T_0, T_1, T_2

Eq. (2.6) yields three pairs of wave modes. For a wave mode $\omega = W(k)$, the group velocity C can be calculated from

$$C = -\frac{\alpha_1' W^4 + \alpha_2' W^2 + \alpha_3'}{6W^5 + 4\alpha_1 W^3 + 2\alpha_2 W} \tag{2.9}$$

in which $\alpha_j' = \mathrm{d}\alpha_j/\mathrm{d}k$.

One mode, T_0, has no cut-off frequency. As $k \to 0$ in the low frequency domain, the dispersion relation for the mode T_0 can be described by

$$\omega \sim 2k\sqrt{\frac{\alpha - 1}{\alpha}} = c_{\mathrm{P}} k \quad \text{then } c, C \sim c_{\mathrm{P}}. \tag{2.10}$$

Note that the normalized plate velocity $c_{\mathrm{P}} = \sqrt{2/(1-\nu)}$ appears both in the classical plate theory and in the 2-D elasticity theory (Lamb waves). Therefore, the low frequency limit of velocity of the mode T_0 is the plate velocity. The eigenvector $\boldsymbol{a}$ corresponding to the mode shows that the displacement field is dominated by $u_r = u\cos\phi + v\sin\phi$, as $k \to 0$. The mode is essentially longitudinal waves, when $k \ll 1$.

Letting $k = 0$ in Eq. (2.6), the cut-off frequencies for other two modes, T_1 and T_2, are given respectively by

$$\omega_c = \sqrt{3\alpha}\kappa (= \pi\sqrt{\alpha}/2), \quad \sqrt{15}\kappa_4 (= \pi). \tag{2.11}$$

Letting $k \to \infty$ in the high frequency domain, the dispersion relation becomes

$$\frac{\omega^2}{k^2} \sim \kappa_4^2, \;\; c, C \sim \kappa_4 = \frac{\pi}{\sqrt{15}}, \quad \text{for } T_0 \text{ mode},$$

$$\frac{\omega^2}{k^2} \sim \alpha, \;\; c, C \sim c_{\mathrm{L}}, \quad \text{for } T_1 \text{ and } T_2 \text{ modes}.$$

The limit, $\pi/\sqrt{15}$ representing the normalized wave velocity of the mode T_0 when $k \to \infty$, is less than 1 (being normalized by c_{T}) and is close to c_{R} ($c_{\mathrm{R}} = 0.932$ for $\nu = 0.33$) being the velocity of Rayleigh waves. The velocities of the modes T_1 and T_2 approach c_{L} which describes the longitudinal waves in a three-dimensional elastic body.

2.2. Flexural waves

For the linear equations Eq. (1.11) with zero loads, the wave elementary solutions for the flexural wave motion $\mathbf{U} = [w, \psi_1, \psi_2]^{\mathrm{T}}$ take the basic form:

$$\mathbf{U} = \boldsymbol{a}\exp[\mathrm{i}(\boldsymbol{k}\cdot\boldsymbol{x} - \omega t)]. \tag{2.12}$$

From Eq. (1.11) and (2.12), we have the matrix equation

$$(\mathbf{A} - \omega^2\mathbf{I})\boldsymbol{a} = \mathbf{0}, \tag{2.13}$$

where

$$\mathbf{A} = \begin{bmatrix} \kappa^2 k^2 & -\mathrm{i}\kappa^2 k_1 & -\mathrm{i}\kappa^2 k_2 \\ 3\mathrm{i}\kappa^2 k_1 & \alpha k_1^2 + k_2^2 + 3\kappa^2 & (\alpha - 1)k_1 k_2 \\ 3\mathrm{i}\kappa^2 k_2 & (\alpha - 1)k_1 k_2 & k_1^2 + \alpha k_2^2 + 3\kappa^2 \end{bmatrix}.$$

The dispersion relation for Eq. (1.11) then follows from the condition that the determinant

$$|\mathbf{A} - \omega^2\mathbf{I}| = 0. \tag{2.14}$$

Eq. (2.14) is a standard eigenvalue problem that can be expanded as

$$\omega^6 + a_1\omega^4 + a_2\omega^2 + a_3 = 0, \tag{2.15}$$

where a_j are related to $\mathbf{A}$. Eq. (2.15) can be further decomposed into two equations:

$$\omega^2 - k^2 - \pi^2/4 = 0, \tag{2.16}$$

$$\omega^4 - [(\alpha+\kappa^2)k^2 + 3\kappa^2]\omega^2 + \alpha\kappa^2k^4 = 0. \tag{2.17}$$

Hence, there are three pairs of wave modes.

From Eqs. (2.16) and (2.17), the frequency ω, phase velocity c and group velocity C can be expressed as

$$\omega^2 = k^2 + \pi^2/4, \quad \frac{(\alpha+\kappa^2)k^2 + 3\kappa^2}{2} \pm \sqrt{\left[\frac{(\alpha-\kappa^2)k^2 + 3\kappa^2}{2}\right]^2 + 3\kappa^4k^2}, \tag{2.18}$$

then

$$c^2 = 1 + \frac{\pi^2}{12k^2}, \quad \frac{(\alpha+\kappa^2) + 3\kappa^2k^{-2}}{2} \pm \sqrt{\left[\frac{(\alpha-\kappa^2) + 3\kappa^2k^{-2}}{2}\right]^2 + 3\kappa^4k^{-2}}, \tag{2.19}$$

$$\mathbf{C} = C\hat{\mathbf{k}}, \tag{2.20}$$

where

$$C = k/\omega, \quad \text{for the wave mode from Eq. (2.16)}, \tag{2.21}$$

$$C = -\frac{2\alpha\kappa^2k^2 - (\alpha+\kappa^2)\omega^2}{2\omega^2 - (\alpha+\kappa^2)k^2 - 3\kappa^2}c^{-1}, \quad \text{for the modes from Eq. (2.17)} \tag{2.22}$$

Fig. 2 shows the group velocity C as a function of the frequency ω for each flexural wave mode for a plate with $\nu = 0.33$. The three modes are labeled as B_0, B_1, and B_2 in Fig. 2. The mode B_2 represents the antisymmetric SH wave. In the following the phase and group velocities in the low and high frequencies are discussed.

Wave mode B_2: $\omega^2 = k^2 + \pi^2/4$

$$C = \frac{k}{\sqrt{k^2 + \pi^2/4}} = \frac{\sqrt{\omega^2 - \pi^2/4}}{\omega}, \quad c = \frac{1}{C}.$$

The mode possesses the following cut-off frequency ω_c as $k \to 0$,

$$\omega_c = \sqrt{3}\kappa = \pi/2,$$

and the wave speeds approach the pure shear waves as $k \to \infty$

$$c, C \sim 1 \quad \text{as } k \to \infty.$$

The displacements for the mode indicate that the mode represents horizontal shear waves. For the antisymmetric SH waves in a plate, the 3-D elasticity provides the following dispersion relation

$$\omega^2 = k^2 + \left(\frac{n\pi}{2}\right)^2, \quad n = 1, 3, 5, \ldots$$

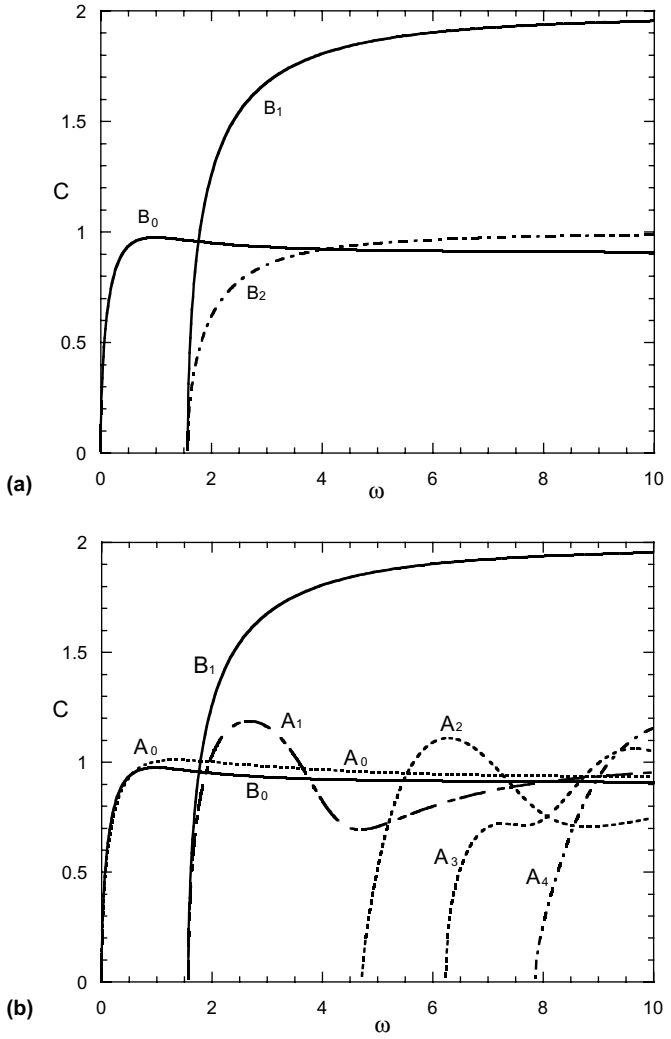

Fig. 2. Group velocity dispersion relation of flexural waves ($v = 0.33$): (a) three modes based on plate theory, (b) axisymmetric wave modes of plate theory and 3-D elasticity.

Thus, the mode B_2 is same as the first SH wave mode of 3-D elasticity. Note that the second SH mode can be also be yielded by the plate theory, if more higher-order terms are included in the bending displacement field.

Wave modes: B_0 and B_1

Eq. (2.17) yields two pairs of flexural wave modes: One mode B_0 without cut-off frequency and the other B_1 with cut-off frequency. For the mode B_0, ω approaches zero as $k \to 0$, and the dispersion relation becomes

$$\omega^2 \sim \frac{\alpha k^4}{3} = \frac{2(1-v)}{3(1-2v)} k^4 \quad \text{as } k \to 0 \tag{2.23}$$

or

$$c \sim \sqrt{\alpha/3}k = (\alpha/3)^{1/4}\sqrt{\omega}, \quad C \sim 2c \quad \text{as } k \to 0.$$

Note that in the low-frequency region the dispersion relation does not approach that for classical plate theory ($\omega^2 = \alpha k^4$ is the dispersion relation of flexural waves for classical plate theory).

Letting $k = 0$ in Eq. (2.17), the cut-off frequency for the B_1 mode is given by

$$\omega_c = \sqrt{3}\kappa = \pi/2.$$

Letting $k \to \infty$, the dispersion relation becomes

$$\frac{\omega^2}{k^2} \sim \kappa^2, \quad c, C \sim \kappa \quad \text{as } k \to \infty \text{ for } B_0 \text{ mode}, \tag{2.24}$$

$$\frac{\omega^2}{k^2} \sim \alpha, \quad c, C \sim c_{\mathrm{L}} \quad \text{as } k \to \infty \text{ for } B_1 \text{ mode}. \tag{2.25}$$

The velocity of the mode B_0 in the high frequency domain, $C \sim \kappa = 0.907$, while $C \sim c_{\mathrm{R}} = 0.932$ for $v = 0.33$ for A_0 mode of 3-D elasticity solution. The limit of velocity of the higher-order mode B_1 is c_{L}.

3. Axisymmetric extensional waves using higher-order plate theory

When an infinite plate is subjected to axisymmetric loads, then all variables are only functions of the radial coordinate r and time t based on the plate theory. The behavior based on the classical plate theory is described in Appendix A. In cylindrical coordinates the plate displacement field for the axisymmetric deformation is

$$\begin{aligned} u_r(r,z,t) &= u(r,t) + z\psi(r,t) + z^2\varphi(r,t), \\ u_3(r,z,t) &= w(r,t) + z\psi_3(r,t), \end{aligned} \tag{3.1}$$

where (u_r, u_3) are the radial and transverse displacements, respectively, ψ is the rotation of a transverse normal about the θ-direction. Since the in-plane extensional wave motion (u, φ, ψ_3) is uncoupled from flexural wave motion (w, ψ) in the linear case, the two types of waves will be discussed separately in this and the following sections.

With the linear strain–displacement relation, the equations of motion of extensional waves can be obtained using the Hamilton's principle, that is,

$$\begin{aligned} &\frac{1}{r}\frac{\partial}{\partial r}(rN_r) - \frac{N_\theta}{r} + q_r = I_0\ddot{u} + I_2\ddot{\varphi}, \\ &\frac{1}{r}\frac{\partial}{\partial r}(rS_r) - \frac{S_\theta}{r} - R_r + n_r = \frac{I_2}{2}\ddot{u} + \frac{I_4}{2}\ddot{\varphi}, \\ &\frac{1}{r}\frac{\partial}{\partial r}(rR_r) - N_z + m = I_2\ddot{\psi}_3. \end{aligned} \tag{3.2}$$

Rewriting the equations of motion in terms of displacements

$$\begin{aligned} &\frac{1}{\rho}(\lambda + 2G)\left(\nabla^2 - \frac{1}{r^2}\right)(I_0 u + I_2\varphi) + \frac{I_0}{\rho}\kappa\lambda\frac{\partial\psi_3}{\partial r} + q_r = I_0\ddot{u} + I_2\ddot{\varphi}, \\ &\frac{1}{\rho}(\lambda + 2G)\left(\nabla^2 - \frac{1}{r^2}\right)(I_2 u + I_4\varphi) + \frac{I_2}{\rho}\left[(\kappa\lambda - 2\kappa_4^2 G)\frac{\partial\psi_3}{\partial r} - 4\kappa_4^2 G\varphi\right] + n_r = I_2\ddot{u} + I_4\ddot{\varphi}, \\ &\frac{I_2}{\rho}\left[\kappa_4^2 G\nabla^2\psi_3 + (2\kappa_4^2 G - \kappa\lambda)\frac{1}{r}\frac{\partial}{\partial r}(r\varphi)\right] - \frac{I_0}{\rho}\left[\kappa\lambda\frac{1}{r}\frac{\partial}{\partial r}(ru) + \kappa^2(\lambda + 2G)\psi_3\right] + m = I_2\ddot{\psi}_3, \end{aligned} \tag{3.3}$$

and using the nondimensional variables and quantities defined by Eq. (1.9), the dimensionless equations of motion become

$$\begin{aligned}
&\alpha\left(\nabla^2-\frac{1}{r^2}\right)\left(u+\frac{1}{3}\varphi\right)+(\alpha-2)\kappa\frac{\partial\psi_3}{\partial r}+q_r=\ddot{u}+\frac{1}{3}\ddot{\varphi},\\
&\alpha\left(\nabla^2-\frac{1}{r^2}\right)\left(\frac{5}{3}u+\varphi\right)+\frac{5}{3}[\kappa(\alpha-2)-2\kappa_4^2]\frac{\partial\psi_3}{\partial r}-\frac{20}{3}\kappa_4^2\varphi+n_r=\frac{5}{3}\ddot{u}+\ddot{\varphi},\\
&\kappa_4^2\nabla^2\psi_3+[2\kappa_4^2-\kappa(\alpha-2)]\frac{1}{r}\frac{\partial}{\partial r}(r\varphi)-3\kappa(\alpha-2)\frac{1}{r}\frac{\partial}{\partial r}(ru)-3\kappa^2\alpha\psi_3+m=\ddot{\psi}_3,
\end{aligned}\tag{3.4}$$

where $\nabla^2=\frac{1}{r}\frac{\partial}{\partial r}(r\frac{\partial}{\partial r})$. The extensional wave in a large plate may be solved by using the Laplace and the Hankel transformations.

Suppose that a distributed and transverse force is suddenly applied on a surface of plate. Then $m\neq 0$, $q\neq 0$. In this case, m yields the extensional waves, and q produces the flexural waves in plates. It is worth noting that, according to the classical plate theory and the Mindlin first-order plate theory, there is no extensional deformation associated with the transverse load. However, the higher-order plate theory which considers the terms, ψ_3 and φ, can account for the extensional motion in plates. For example, if an impulse transverse load q^+ is applied on the top surface of the plate, we have $m=3q^+$ via nondimensionalization.

For other loads the problem can be treated in a similar manner. Consider that m is the only nonzero load and the initial conditions are zero. Applying the Laplace and the first-order Hankel transforms to the first two equations in Eq. (3.4), applying the Laplace and the zero-order Hankel transform to the third equation in Eq. (3.4), and defining the following transformed variables:

$$\begin{aligned}
\tilde{\bar{u}}(k,s)&=\int_0^\infty \exp(-st)\,\mathrm{d}t\int_0^\infty rJ_1(kr)u(r,t)\,\mathrm{d}r,\\
\tilde{\bar{\varphi}}(k,s)&=\int_0^\infty \exp(-st)\,\mathrm{d}t\int_0^\infty rJ_1(kr)\varphi(r,t)\,\mathrm{d}r,\\
\tilde{\bar{\psi}}_3(k,s)&=\int_0^\infty \exp(-st)\,\mathrm{d}t\int_0^\infty rJ_0(kr)\psi_3(r,t)\,\mathrm{d}r,\\
\tilde{\bar{m}}(k,s)&=\int_0^\infty \exp(-st)\,\mathrm{d}t\int_0^\infty rJ_0(kr)m(r,t)\,\mathrm{d}r,
\end{aligned}\tag{3.5}$$

where s is the Laplace transform parameter, k the Hankel transform parameter, $\tilde{u},\bar{u},\tilde{\bar{u}},\ldots$ are the Hankel transform, Laplace transform, and the joint Hankel and Laplace transform of function u, respectively, …, $J_n(kr)$ is the Bessel function of order n. Then Eq. (3.4) can be transformed into

$$(\mathbf{T}+s^2\mathbf{M})\tilde{\bar{\mathbf{U}}}=\tilde{\bar{m}}\mathbf{I}_3,\tag{3.6}$$

where $\tilde{\bar{\mathbf{U}}}=[\tilde{\bar{u}},\tilde{\bar{\varphi}},\tilde{\bar{\psi}}_3]^{\mathrm{T}}$, $\mathbf{I}_3=[0,0,1]^{\mathrm{T}}$,

$$\mathbf{T}=\begin{bmatrix}\alpha k^2 & \alpha k^2/3 & \kappa(\alpha-2)k\\ \frac{5}{3}\alpha k^2 & \alpha k^2+\frac{20}{3}\kappa_4^2 & \frac{5}{3}[\kappa(\alpha-2)-2\kappa_4^2]k\\ 3\kappa(\alpha-2)k & [\kappa(\alpha-2)-2\kappa_4^2]k & \kappa_4^2k^2+3\alpha\kappa^2\end{bmatrix},\quad \mathbf{M}=\begin{bmatrix}1 & 1/3 & 0\\ 5/3 & 1 & 0\\ 0 & 0 & 1\end{bmatrix}.\tag{3.7}$$

Eq. (3.7) is reached by employing the following operational properties of the Hankel transform (Debnath, 1995)

$$\int_0^\infty rJ_0(kr)\nabla^2 f(r)\,\mathrm{d}r=-k^2\tilde{f}_0(k),\quad \text{the zero-order Hankel transform,}$$

$$\int_0^\infty rJ_1(kr)\left(\nabla^2-\frac{1}{r^2}\right)f(r)\,\mathrm{d}r=-k^2\tilde{f}_1(k),\quad \text{the first-order Hankel transform,}$$

$$H_0\left\{\frac{1}{r}\frac{\mathrm{d}}{\mathrm{d}r}[rf(r)]\right\}=kH_1\{f(r)\}\equiv k\tilde{f}_1(k),\quad H_1\{f'(r)\}=-kH_0\{f(r)\}=-k\tilde{f}_0(k)$$

provided $rf(r)\to 0$ as $r\to 0$ and ∞, where H_j is the Hankel transform operator and the subscript j is the transform order.

The solution of Eq. (3.6) is

$$\tilde{\overline{\mathbf{U}}}=(\mathbf{T}+s^2\mathbf{M})^{-1}\tilde{\bar{m}}\mathbf{I}_3=\frac{\mathrm{adj}(\mathbf{T}+s^2\mathbf{M})}{|\mathbf{T}+s^2\mathbf{M}|}\tilde{\bar{m}}\mathbf{I}_3. \tag{3.8}$$

Note that the denominator can be expressed as

$$|\mathbf{T}+s^2\mathbf{M}|=(s^2+s_1^2)(s^2+s_2^2)(s^2+s_3^2),$$

where s_1^2, s_2^2, and s_3^2 are the roots of the equation, $|\mathbf{T}+s^2\mathbf{M}|=0$.

By introducing the substitution $s=\mathrm{i}\omega$, the equation $|\mathbf{T}+s^2\mathbf{M}|=0$ becomes

$$|\mathbf{T}-\omega^2\mathbf{M}|=0. \tag{3.9}$$

Eq. (3.9) is recognized as the dispersion relation presented earlier by Eq. (2.6). Thus, here ω represents the frequency and k, the Hankel transform variable, represents the wave number. The eigenvalues ω^2 in Eq. (3.9) may be expressed in the form

$$\omega^2=W_1^2(\mathbf{k}),W_2^2(\mathbf{k}),W_2^2(\mathbf{k}).$$

Therefore, there are three extensional wave modes, T_0, T_1, and T_2, in a plate under axisymmetric deformation according to the higher-order plate theory. The dispersion relation is shown by the solid lines in Fig. 1(a), where the group velocity C varies with frequency ω.

Since $s_1^2=-W_1^2$, $s_2^2=-W_2^2$, $s_3^2=-W_3^2$, Eq. (3.8) can be rewritten as

$$\tilde{\overline{\mathbf{U}}}=\frac{\mathrm{adj}(T+s^2\mathbf{M})}{(s^2+W_1^2)(s^2+W_2^2)(s^2+W_3^2)}\tilde{\bar{m}}\mathbf{I}_3. \tag{3.10a}$$

The next step is to take the inverse Laplace transform. In order to successfully determine the inverse Laplace transform to Eq. (3.10a), $\overline{\mathbf{U}}(\mathbf{k},s)$ needs to be expressed as the sum of terms $1/(s^2+W_j^2)$ and/or $s/(s^2+W_j^2)$.

Decomposition of $\tilde{\overline{\mathbf{U}}}(\mathbf{k},s)$ in Eq. (3.10a) gives

$$\tilde{\overline{\mathbf{U}}}=\mathbf{A}_\mathrm{T}\begin{Bmatrix}(s^2+W_1^2)^{-1}\\(s^2+W_2^2)^{-1}\\(s^2+W_3^2)^{-1}\end{Bmatrix}\tilde{\bar{m}}, \tag{3.10b}$$

where $\mathbf{A}_\mathrm{T}(k)$ can be determined from Eqs. (3.10a) and (3.10b), and may be expressed in the form

$$\mathbf{A}_\mathrm{T}=\mathbf{D}_\mathrm{T}\boldsymbol{\Omega}^{-1}, \tag{3.11}$$

$$\mathbf{D}_\mathrm{T}=\begin{bmatrix}0 & m_{12}T_{23}-T_{13} & T_{12}T_{23}-T_{22}T_{13}\\ 0 & m_{21}T_{13}-T_{23} & T_{21}T_{13}-T_{11}T_{23}\\ 1-m_{12}m_{21} & T_{11}+T_{22}-m_{12}T_{21}-m_{21}T_{12} & T_{11}T_{22}-T_{12}T_{21}\end{bmatrix},$$

$$\mathbf{\Omega} = \begin{bmatrix} 1 & W_2^2 + W_3^2 & W_2^2 W_3^2 \\ 1 & W_3^2 + W_1^2 & W_3^2 W_1^2 \\ 1 & W_1^2 + W_2^2 & W_1^2 W_2^2 \end{bmatrix},$$

where T_{ij} and m_{ij} are the elements of the **T** and **M** matrices in Eq. (3.9) respectively.

Applying the inverse Laplace transform to Eq. (3.10b) yields

$$\widetilde{\mathbf{U}}(\mathbf{k}, t) = \mathbf{A}_{\mathrm{T}} \int_0^t \begin{Bmatrix} W_1^{-1} \sin W_1(t-\xi) \\ W_2^{-1} \sin W_2(t-\xi) \\ W_3^{-1} \sin W_3(t-\xi) \end{Bmatrix} \tilde{m}(k, \xi)\, \mathrm{d}\xi. \tag{3.12}$$

Eq. (3.12) is derived by using the inverse Laplace transform (Debnath, 1995)

$$L^{-1}\left\{\frac{1}{s^2 + W_i^2}\right\} = \frac{\sin W_i t}{W_i}$$

and the convolution theorem

$$L^{-1}\left\{\frac{1}{s^2 + W_i^2}\tilde{\tilde{q}}(k, s)\right\} = \int_0^t \frac{\sin W_i(t-\xi)}{W_i} \tilde{q}(k, \xi)\, \mathrm{d}\xi.$$

The inverse Hankel transform of $\widetilde{\mathbf{U}}$ in Eq. (3.12) leads to

$$\begin{Bmatrix} u \\ \varphi \\ \psi_3 \end{Bmatrix} = \int_0^\infty k\, \mathrm{diag}[J_1(kr), J_1(kr), J_0(kr)] \mathbf{A}_{\mathrm{T}} \mathbf{H}(t, k)\, \mathrm{d}k, \tag{3.13}$$

$$\mathbf{H} = [h_1, h_2, h_3]^{\mathrm{T}}, \qquad h_i(t, k) = W_i^{-1} \int_0^t \sin W_i(t-\xi) \tilde{m}(k, \xi)\, \mathrm{d}\xi, \quad i = 1, 2, 3. \tag{3.14}$$

In general, a point load applied at the center of the plate may be written as

$$m = \frac{m_0}{2\pi} \frac{\delta(r)}{r} f(t),$$

here m_0 is the magnitude of the applied load. Then

$$h_i(t, k) = \frac{m_0}{2\pi W_i} \int_0^t f(\xi) \sin W_i(t-\xi)\, \mathrm{d}\xi, \quad i = 1, 2, 3.$$

The expressions for $h_i(t,k)$ for some specific point loads with $m_0 = 1$ are given below

(a) Pure impulse load

Consider a pure impulse point load, $f(t) = \delta(t)$, where $\delta(t)$ is a Dirac delta function, then

$$h_i(t, k) = \frac{\sin W_i t}{2\pi W_i}. \tag{3.15}$$

Eq. (3.13) becomes

$$\begin{Bmatrix} u(r, t) \\ \varphi(r, t) \\ \psi_3(r, t) \end{Bmatrix} = \frac{1}{2\pi} \int_0^\infty k\, \mathrm{diag}[J_1(kr), J_1(kr), J_0(kr)] \mathbf{A}_{\mathrm{T}} \begin{Bmatrix} W_1^{-1} \sin W_1 t \\ W_2^{-1} \sin W_2 t \\ W_3^{-1} \sin W_3 t \end{Bmatrix} \mathrm{d}k. \tag{3.16}$$

If the impulse load is located at $\mathbf{r}' = (r', \theta')$, $f(t) = \delta(t - t')$, from Eq. (3.13) and the transformation of the displacements, the solutions at $\mathbf{r} = (r, \theta)$ may be rewritten as

$$\begin{aligned} &u_r(\mathbf{r}, t; \mathbf{r}', t') = u' \cos(\theta' - \theta), \quad u_\theta(\mathbf{r}, t; \mathbf{r}', t') = u' \sin(\theta' - \theta), \\ &\varphi_r(\mathbf{r}, t; \mathbf{r}', t') = \varphi' \cos(\theta' - \theta), \quad \varphi_\theta(\mathbf{r}, t; \mathbf{r}', t') = \varphi' \sin(\theta' - \theta), \\ &\psi_3(\mathbf{r}, t; \mathbf{r}', t') = \psi_3', \end{aligned} \tag{3.17}$$

with

$$\begin{Bmatrix} u' \\ \varphi' \\ \psi_3' \end{Bmatrix} = \frac{1}{2\pi} \int_0^\infty k \begin{bmatrix} J_1(k|\mathbf{r} - \mathbf{r}'|) & 0 & 0 \\ 0 & J_1(k|\mathbf{r} - \mathbf{r}'|) & 0 \\ 0 & 0 & J_0(k|\mathbf{r} - \mathbf{r}'|) \end{bmatrix} \mathbf{A}_\mathrm{T} \begin{Bmatrix} W_1^{-1} \sin W_1(t - t') \\ W_2^{-1} \sin W_2(t - t') \\ W_3^{-1} \sin W_3(t - t') \end{Bmatrix} \mathrm{d}k. \tag{3.18}$$

These solutions are the Green's functions for extensional waves describing the response at r and t to a unit impulse load m applied at r' and $t = t'$.

(b) N-peak signal

Assume a point load at $r = 0$ can be described by a narrow-band N-peak signal, i.e.,

$$f(t) = \left[H(t) - H\left(t - \frac{2\pi N}{p}\right)\right]\left(1 - \cos\frac{pt}{N}\right)\sin pt \quad (N = 3, 5, 7, \ldots),$$

where p is the central frequency and $H(t)$ is the Heaviside unit step function. Obviously, the loading duration is $T = 2\pi N/p$.

From Eq. (3.14), h_i for $t > T$ is given by

$$\begin{aligned} &h_i = \frac{1}{2\pi W_i}\left[\frac{p}{p^2 - W_i^2} - \frac{1}{2}\left(\frac{p_1}{p_1^2 - W_i^2} + \frac{p_2}{p_2^2 - W_i^2}\right)\right][(1 - \cos W_i T)\sin W_i t + \sin W_i T \cos W_i t], \\ &p_1 = p(N - 1)/N, \;\; p_2 = p(N + 1)/N, \end{aligned}$$

(c) Step-function loading

$$f(t) = H(t).$$

Eq. (3.14) leads to

$$h_i = \frac{(1 - \cos W_i t)}{2\pi W_i^2}.$$

(d) Rectangular impulse

$$f(t) = H(t) - H(t - T).$$

Considering $t > T$, Eq. (3.14) gives

$$h_i = \frac{\sin W_i T/2}{2\pi W_i^2} \sin W_i(t - T/2).$$

(e) Half-sine-wave impulse

$$f(t) = [H(t) - H(t-T)]\sin pt,$$

where T is the duration of load, $T = \pi/p$.

$$h_i = \frac{p\cos W_i T/2}{\pi W_i(p^2 - W_i^2)}\sin W_i(t - T/2), \quad t > T.$$

With the expressions $h_i(t,k)$ for different loads given above, Eq. (3.13) indicates that the inverse Hankel transform in $0 < k < \infty$ for the pure impulse load converges slower than those for other loads if numerical evaluation is employed. This can be seen from the following observation. As $k \to \infty$, the integrand in Eq. (3.13) approaches $k^{-\gamma}$ ($\gamma > 0$) for any load, and the value of γ for $f(t) = \delta(t)$ is minimum among all the loads.

3.1. Asymptotic expansion

These integrals in Eq. (3.13) represent exact solutions for u, φ, and ψ_3 at any r and t. It is usually unlikely to evaluate them exactly. The alternatives are numerical evaluation, or an approximate analytical evaluation. However, the numerical evaluation is not convenient to describe the physical features of the wave motions. In order to resolve this difficulty, it is necessary and useful to resort to asymptotic methods. It will be sufficient for determination of the basic features of the wave motions to evaluate Eq. (3.13) asymptotically for large times and large distances with r/t held fixed. Replacing $J_0(kr)$ and $J_1(kr)$ by their asymptotic expansions for $kr \to \infty$ in Eq. (3.13),

$$\begin{aligned} J_0(kr) &\sim \sqrt{\frac{2}{\pi kr}}\cos(kr - \pi/4), \\ J_1(kr) &\sim \sqrt{\frac{2}{\pi kr}}\sin(kr - \pi/4), \end{aligned} \tag{3.19}$$

and applying the stationary phase to the integrals for large values of t (Stamnes, 1986; Jeffreys and Jefferys, 1956), the asymptotic expansion can be obtained. For example, for the pure impulsive point load Eq. (3.13) becomes

$$\begin{aligned} u(r,t) &\sim \frac{1}{2\pi\sqrt{2\pi r}}\sum_i \int_0^\infty F_{1i}(k)\mathrm{Re}\{\exp[\mathrm{i}(kr - W_i t - \pi/4)]\}\,\mathrm{d}k, \\ \varphi(r,t) &\sim \frac{1}{2\pi\sqrt{2\pi r}}\sum_i \int_0^\infty F_{2i}(k)\mathrm{Re}\{\exp[\mathrm{i}(kr - W_i t - \pi/4)]\}\,\mathrm{d}k, \\ \psi_3(r,t) &\sim \frac{1}{2\pi\sqrt{2\pi r}}\sum_i \int_0^\infty F_{3i}(k)\mathrm{Re}\{\exp[\mathrm{i}(kr - W_i t + \pi/4)]\}\,\mathrm{d}k, \end{aligned} \tag{3.20}$$

as $kr \to \infty$, where the expressions for F_{ij} can be readily obtained from Eq. (3.13) after matrix manipulation. Further, for large values of t the stationary phase method gives

$$\begin{aligned} u(r,t) &\sim \frac{1}{2\pi\sqrt{rt}}\mathrm{Re}\sum_i \sum_{\substack{\text{stationary} \\ \text{points } k}} \frac{F_{1i}(k)}{\sqrt{|W_i''|}}\exp \mathrm{i}[kr - W_i t - \pi(1 + \operatorname{sgn} W_i'')/4], \\ \varphi(r,t) &\sim \frac{1}{2\pi\sqrt{rt}}\mathrm{Re}\sum_i \sum_{\substack{\text{stationary} \\ \text{points } k}} \frac{F_{2i}(k)}{\sqrt{|W_i''|}}\exp \mathrm{i}[kr - W_i t - \pi(1 + \operatorname{sgn} W_i'')/4], \\ \varphi_3(r,t) &\sim \frac{1}{2\pi\sqrt{rt}}\mathrm{Re}\sum_i \sum_{\substack{\text{stationary} \\ \text{points } k}} \frac{F_{3i}(k)}{\sqrt{|W_i''|}}\exp \mathrm{i}[kr - W_i t + \pi(1 - \operatorname{sgn} W_i'')/4], \end{aligned} \tag{3.21}$$

where sgn stands for sign function and $k = k(r,t)$ is the stationary point which is root of the equations

$$W_i'(k) = \frac{r}{t}, \quad k > 0 \text{ and } \frac{r}{t} > 0 \quad (i = 1,2,3). \tag{3.22}$$

Eq. (3.21) indicates that the amplitude is proportional to $(rt)^{-1/2}$. The approximation provided by the stationary phase breaks down near points where $W_i'' = 0$.

In this case, a proper asymptotic approximation can be constructed by expanding the exponent in Eq. (3.20) around k_0 where $W_i''(k_0) = 0$, and retaining up to third-order terms. Then the transitional Airy approximation in the region can be obtained (Stamnes, 1986; Achenbach, 1984). Again, for the pure impulsive point load the asymptotic solutions are

$$\begin{aligned}
u(r,t) &\sim \frac{\mathrm{Re}}{\sqrt{2\pi r}(t/2)^{1/3}} \sum_i \sum_{\substack{\text{stationary} \\ \text{points } k}} F_{1i}(k) \frac{Ai(z_i)}{|W_i'''|^{1/3}} \exp[\mathrm{i}(kr - W_i t - \pi/4)], \\
\varphi(r,t) &\sim \frac{\mathrm{Re}}{\sqrt{2\pi r}(t/2)^{1/3}} \sum_i \sum_{\substack{\text{stationary} \\ \text{points } k}} F_{2i}(k) \frac{Ai(z_i)}{|W_i'''|^{1/3}} \exp[\mathrm{i}(kr - W_i t - \pi/4)], \\
\psi_3(r,t) &\sim \frac{\mathrm{Re}}{\sqrt{2\pi r}(t/2)^{1/3}} \sum_i \sum_{\substack{\text{stationary} \\ \text{points } k}} F_{3i}(k) \frac{Ai(z_i)}{|W_i'''|^{1/3}} \exp[\mathrm{i}(kr - W_i t + \pi/4)],
\end{aligned} \tag{3.23}$$

where

$$z_i = \mathrm{sgn}(W_i''') \frac{W_i' t - x}{(|W_i'''| t/2)^{1/3}}$$

$Ai(x)$ is the Airy function, and its integral representation is

$$Ai(x) = \frac{1}{\pi} \int_0^\infty \cos\left(xs + \frac{1}{3}s^3\right) \mathrm{d}s$$

In the Airy expansion, k should be understood that $k = k_0$, the stationary point of group velocity. Eq. (3.23) shows that the wave amplitude varies as $t^{-1/3} r^{-1/2}$. Hence, the predominant contribution comes from the neighborhood of k_0. For instance, the wave mode T_0 indicates

$$W(k) \sim c_P k - \varsigma k^3, \quad W''(k) \sim 0, \text{ as } k \to 0,$$

here $c_P = \sqrt{2/(1-\nu)}$ is the normalized plate velocity, $\varsigma = \text{constant} > 0$, the stationary phase is not valid in the neighborhood of $k = 0$. However, the correct expansion in the transition region can be constructed by the Airy approximation. The asymptotic results show that the contribution from the mode decays exponentially ahead of the curve $r = c_P t$ and becomes oscillatory behind the curve. The asymptotic solutions for other loads can be obtained in a similar manner.

As $k \to \infty$, $W'(k)$ or group velocity reaches plateau, and $W''(k), W'''(k), \ldots$, approach zero for all the modes. In this case, asymptotic expansions based on the stationary phase and the Airy approximation are invalid. However, the integral over the interval (k_f, ∞) $(k_f \gg 1)$, $r^{-1/2} \int_{k_f}^\infty F(k) \exp[\mathrm{i}(kr - Wt)] \mathrm{d}k$, can be simplified significantly. It represents rapid oscillations trend to cancel contributions to the entire integral, and its magnitude is of order smaller than $(rt)^{-1/2}$, if the asymptotic expansion of $W(k)$ is applied. This conclusion can also be used to estimate the error incurred by replacing the interval $(0,\infty)$ with $(0,k_f)$ in the numerical calculation.

4. Axisymmetric flexural waves using higher-order plate theory

We begin with the following flexural displacement field for the Reissner–Mindlin plate theory,

$$\begin{aligned} u_r(r,z,t) &= z\psi(r,t), \\ u_3(r,z,t) &= w(r,t). \end{aligned} \tag{4.1}$$

The governing equations without nondimensionalization are given by

$$\begin{aligned} &\frac{1}{r}\frac{\partial}{\partial r}(rQ_r) + q = I_0\ddot{w}, \\ &\frac{1}{r}\left[\frac{\partial}{\partial r}(rM_r) - M_\theta\right] - Q_r = I_2\ddot{\psi}. \end{aligned} \tag{4.2}$$

The plate constitutive relations are

$$\begin{aligned} M_r &= \left[(\lambda+2G)\frac{\partial\psi}{\partial r} + \lambda\frac{\psi}{r}\right]\frac{h^3}{12}, \\ M_\theta &= \left[\lambda\frac{\partial\psi}{\partial r} + (\lambda+2G)\frac{\psi}{r}\right]\frac{h^3}{12}, \\ Q_r &= \kappa^2 G\left(\psi + \frac{\partial w}{\partial r}\right)h. \end{aligned} \tag{4.3}$$

The dimensionless displacement equations of motion for flexural waves in an isotropic plate with transverse load $q(\mathbf{x},t)$ and zero initial conditions take the form (note the nondimensional quantities are shown by Eq. (1.11), and the "primes" on the dimensionless quantities are dropped)

$$\begin{aligned} &\ddot{w} - \kappa^2\nabla^2 w - \frac{\kappa^2}{r}\frac{\partial}{\partial r}(r\psi) = q, \quad t>0, \\ &\ddot{\psi} + 3\kappa^2\left(\psi + \frac{\partial w}{\partial r}\right) - \alpha\left(\nabla^2 - \frac{1}{r^2}\right)\psi = 0, \end{aligned} \tag{4.4}$$

$$\mathbf{U} = \frac{\partial\mathbf{U}}{\partial t} = \mathbf{0} \quad \text{at } t=0, \tag{4.5}$$

where $\nabla^2 = \frac{1}{r}\frac{\partial}{\partial r}\left(r\frac{\partial}{\partial r}\right)$, $\mathbf{U} = [w,\psi]^{\mathrm{T}}$.

In a similar approach to the extensional waves, the flexural wave in the plate can be solved by using the Laplace and the Hankel transformations. Applying the Laplace and the zero-order Hankel transform to the first equation in Eq. (4.4), while applying the Laplace and the first-order Hankel transform to the second equation in Eq. (4.4), and then defining the following transformed variables

$$\begin{aligned} \tilde{\bar{w}}(k,s) &= \int_0^\infty \exp(-st)\,\mathrm{d}t\int_0^\infty rJ_0(kr)w(r,t)\,\mathrm{d}r, \\ \tilde{\bar{\psi}}(k,s) &= \int_0^\infty \exp(-st)\,\mathrm{d}t\int_0^\infty rJ_1(kr)\psi(r,t)\,\mathrm{d}r, \\ \tilde{\bar{q}}(k,s) &= \int_0^\infty \exp(-st)\,\mathrm{d}t\int_0^\infty rJ_0(kr)q(r,t)\,\mathrm{d}r. \end{aligned} \tag{4.6}$$

Eqs. (4.4) and (4.5) are transformed into

$$(\mathbf{B} + s^2\mathbf{I})\tilde{\bar{\mathbf{U}}} = \tilde{\bar{q}}\mathbf{I}_1 \tag{4.7}$$

where $\widetilde{\widetilde{\mathbf{U}}} = [\tilde{\tilde{w}}, \tilde{\tilde{\psi}}]^{\mathrm{T}}$, $\boldsymbol{I}_1 = [1,0]^{\mathrm{T}}$,

$$\mathbf{B} = \begin{bmatrix} \kappa^2 k^2 & -\kappa^2 k \\ -3\kappa^2 k & \alpha k^2 + 3\kappa^2 \end{bmatrix}. \tag{4.8}$$

The solution of Eq. (4.7) is

$$\widetilde{\widetilde{\mathbf{U}}} = (\mathbf{B} + s^2\mathbf{I})^{-1}\tilde{\tilde{q}}\mathbf{I}_1$$

or

$$\widetilde{\widetilde{\mathbf{U}}} = \frac{\mathrm{adj}(\mathbf{B} + s^2\mathbf{I})}{|\mathbf{B} + s^2\mathbf{I}|}\tilde{\tilde{q}}\mathbf{I}_1 = \frac{\mathrm{adj}(\mathbf{B} + s^2\mathbf{I})}{(s^2 + s_1^2)(s^2 + s_2^2)}\tilde{\tilde{q}}\mathbf{I}_1, \tag{4.9}$$

where s_1^2 and s_2^2 are the roots of the equation, $|\mathbf{B} + s^2\mathbf{I}| = 0$. Letting $s = \mathrm{i}\omega$, the equation $|\mathbf{B} + s^2\mathbf{I}| = 0$ becomes

$$|\mathbf{B} - \omega^2\mathbf{I}| = 0. \tag{4.10}$$

Eq. (4.10) is identical to the dispersion relation of the plate given by Eq. (2.17). Hence, ω represents the frequency, and k, the Hankel transform variable, represents the wave number here. The eigenvalues ω^2 in Eq. (4.10) may be expressed in the form

$$\omega^2 = W_1^2(\mathbf{k}), W_2^2(\mathbf{k}).$$

The expressions for W_j^2 are given by the last two equations in Eq. (2.18).

Eq. (4.10) indicates that there are two flexural wave modes, B_0 and B_1, in a plate subjected to axisymmetric deformation based on the plate theory. The dispersion relation is shown by the solid lines in Fig. 2(b), where the group velocity C varies as a function of the frequency ω.

With $s_1^2 = -W_1^2$, $s_2^2 = -W_2^2$, decomposition of $\widetilde{\widetilde{\mathbf{U}}}(\mathbf{k}, s)$ in Eq. (4.9) gives

$$\widetilde{\widetilde{\mathbf{U}}} = \frac{\mathrm{adj}(\mathbf{B} + s^2\mathbf{I})}{(s^2 + W_1^2)(s^2 + W_2^2)}\mathbf{I}_1\tilde{\tilde{q}} = \mathbf{A}_b\begin{Bmatrix} (s^2 + W_1^2)^{-1} \\ (s^2 + W_2^2)^{-1} \end{Bmatrix}\tilde{\tilde{q}} \tag{4.11}$$

or

$$\tilde{\tilde{w}} = \left(\frac{a_{11}}{s^2 + W_1^2} + \frac{a_{12}}{s^2 + W_2^2}\right)\tilde{\tilde{q}},$$

$$\tilde{\tilde{\psi}} = \left(\frac{a_{21}}{s^2 + W_1^2} + \frac{a_{22}}{s^2 + W_2^2}\right)\tilde{\tilde{q}},$$

where $\mathbf{A}_b\,(k, W_j) = [a_{ij}]$ can be determined from Eq. (4.11) and may be expressed in the following compact form

$$\mathbf{A}_b = \mathbf{C}_f\boldsymbol{\Omega}^{-1} \tag{4.12}$$

$$\mathbf{C}_f = \begin{bmatrix} 1 & \alpha k^2 + 3\kappa^2 \\ 0 & 3\kappa^2 k \end{bmatrix}, \tag{4.13}$$

$$\boldsymbol{\Omega} = \begin{bmatrix} 1 & W_2^2 \\ 1 & W_1^2 \end{bmatrix}, \tag{4.14}$$

$$\mathbf{A}_b = \frac{1}{W_1^2 - W_2^2}\begin{bmatrix} W_1^2 - \alpha k^2 - 3\kappa^2 & -W_2^2 + \alpha k^2 + 3\kappa^2 \\ -3\kappa^2 k & 3\kappa^2 k \end{bmatrix}.$$

Applying the inverse Laplace transform to Eq. (4.11) gives

$$\widetilde{\mathbf{U}}(\mathbf{k},t) = L^{-1}\left\{\mathbf{A}_b\begin{Bmatrix}(s^2+W_1^2)^{-1}\\(s^2+W_2^2)^{-1}\end{Bmatrix}\tilde{\tilde{q}}(\mathbf{k},s)\right\} = \mathbf{A}_b\int_0^t\begin{Bmatrix}W_1^{-1}\sin W_1(t-\xi)\\W_2^{-1}\sin W_2(t-\xi)\end{Bmatrix}\tilde{q}(k,\xi)\,\mathrm{d}\xi.$$

The inverse Hankel transform of Eq. (4.16) gives

$$\mathbf{U}(r,t) = \int_0^\infty k\,\mathrm{diag}[J_0(kr),J_1(kr)]\mathbf{A}_b\,\mathrm{d}k\int_0^t\begin{Bmatrix}W_1^{-1}\sin W_1(t-\xi)\\W_2^{-1}\sin W_2(t-\xi)\end{Bmatrix}\tilde{q}(k,\xi)\,\mathrm{d}\xi. \tag{4.15}$$

If the load $q(r,t)$ can be separated as $q(r,t) = p(r)f(t)$, then

$$\bar{q} = p(r)\bar{f}(s), \quad \tilde{\bar{q}} = \tilde{p}(k)\bar{f}(s),$$

$$\mathbf{U}(r,t) = \int_0^\infty k\tilde{p}(k)\,\mathrm{diag}[J_0(kr),J_1(kr)]\mathbf{A}_b\,\mathrm{d}k\int_0^t\begin{Bmatrix}W_1^{-1}\sin W_1(t-\xi)\\W_2^{-1}\sin W_2(t-\xi)\end{Bmatrix}f(\xi)\,\mathrm{d}\xi. \tag{4.16}$$

For a point load concentrated at $(0,0)$, $q(r,t)$ can be expressed as $q = \frac{Q_0}{2\pi}\frac{\delta(r)}{r}f(t)$, where Q_0 is the magnitude of the load and $\delta(r)$ is the Dirac delta function. Since $\tilde{p}(k) = \int_0^\infty rJ_0(kr)p(r)\,\mathrm{d}r = \frac{1}{2\pi}$, Eq. (4.16) further reduces to

$$\mathbf{U}(r,t) = \int_0^\infty k\,\mathrm{diag}[J_0(kr),J_1(kr)]\mathbf{A}_b\mathbf{H}(t,k)\,\mathrm{d}k, \tag{4.17}$$

where

$$\mathbf{H}(t,k) = [h_1,h_2]^{\mathrm{T}}, \quad h_i(t,k) = \frac{Q_0}{2\pi W_i}\int_0^t f(\xi)\sin W_i(t-\xi)\,\mathrm{d}\xi, \quad i = 1,2.$$

For the point loads with simple time functions $f(t)$, the expressions for $h_f(t,k)$ are exactly the same as those given in the section of extensional waves.

In general, Eqs. (4.15)–(4.17), can be used to evaluate the flexural wave solution for any form of dynamic loading; however, for arbitrary loadings the evaluation must be performed numerically. For impulsive loads which can be expressed by simple analytical functions, closed form solutions of the equations of motion can be obtained by using Eq. (4.15), or (4.16), or (4.17).

Using asymptotic methods, it will be useful for determination of the basic features of the wave motions to evaluate Eq. (4.17) asymptotically for large times and large distances with r/t held fixed. Using the expansion of the Bessel functions and the stationary phase method, the asymptotic expansion of Eq. (4.17) can be obtained in a similar manner as the extensional waves.

For the pure impulse load, $f(t) = \delta(t)$, the solution is given below:

$$\begin{Bmatrix}w(r,t)\\\psi(r,t)\end{Bmatrix} = \frac{1}{2\pi}\int_0^\infty k\,\mathrm{diag}[J_0(kr),J_1(kr)]\mathbf{A}_b\begin{Bmatrix}W_1^{-1}\sin W_1 t\\W_2^{-1}\sin W_2 t\end{Bmatrix}\mathrm{d}k \tag{4.18}$$

If the pure impulse load is located at $\mathbf{r}' = (r',\theta')$, $f(t) = \delta(t-t')$, with Eq. (4.18), the solution at $\mathbf{r} = (r,\theta)$ may be rewritten as

$$\begin{bmatrix}w(\mathbf{r},t;\mathbf{r}',t')\\\psi_r(\mathbf{r},t;\mathbf{r}',t')\\\psi_\theta(\mathbf{r},t;\mathbf{r}',t')\end{bmatrix} = \begin{bmatrix}1 & 0\\0 & \cos(\theta'-\theta)\\0 & \sin(\theta'-\theta)\end{bmatrix}\begin{Bmatrix}w'\\\psi'\end{Bmatrix} \tag{4.19}$$

with

$$\begin{Bmatrix} w'(\mathbf{r},t) \\ \psi'(\mathbf{r},t) \end{Bmatrix} = \int_0^\infty k \begin{bmatrix} J_0(k|\mathbf{r}-\mathbf{r}'|) & 0 \\ 0 & J_1(k|\mathbf{r}-\mathbf{r}'|) \end{bmatrix} \mathbf{A}_b \begin{Bmatrix} W_1^{-1}\sin W_1(t-t') \\ W_2^{-1}\sin W_2(t-t') \end{Bmatrix} \mathrm{d}k. \tag{4.20}$$

The solution is the Green's functions for flexural waves describing the response at r and t to a unit pure impulse load q applied at r' and $t = t'$.

5. Exact axisymmetric wave solutions of 3-D elasticity theory

For comparison with the higher-order plate theory, the wave behavior under axisymmetric deformation in an isotropic plate provided by "exact" three-dimensional elasticity is derived below. The displacement equations of motion in cylindrical coordinates are

$$\begin{aligned} &(\lambda+2G)\left(\nabla^2 u - \frac{u}{r^2}\right) + G\frac{\partial^2 u}{\partial z^2} + (\lambda+G)\frac{\partial^2 w}{\partial r \partial z} + F_r = \rho\ddot{u}, \\ &G\nabla^2 w + (\lambda+2G)\frac{\partial^2 w}{\partial z^2} + (\lambda+G)\frac{1}{r}\frac{\partial^2 (ru)}{\partial z \partial r} + F_z = \rho\ddot{w}, \end{aligned} \tag{5.1}$$

where u and w are the displacement components in the r and z directions, respectively, F_r, and F_z the body forces. Introducing the length scale $h/2$ and time scale $h/(2c_\mathrm{T})$, and defining the dimensionless variables

$$r' = \frac{r}{h/2}, \quad z' = \frac{z}{h/2}, \quad t' = \frac{t}{h/(2c_\mathrm{T})}, \quad u' = \frac{u}{h/2}, \quad w' = \frac{w}{h/2}, \quad F_i' = \frac{F_i}{2G/h}.$$

The dimensionless equations of motion follow from Eq. (5.1), dropping the primes, as

$$\begin{aligned} &\alpha\left(\nabla^2 u - \frac{u}{r^2}\right) + \frac{\partial^2 u}{\partial z^2} + (\alpha-1)\frac{\partial^2 w}{\partial r \partial z} + F_r = \ddot{u}, \\ &\nabla^2 w + \alpha\frac{\partial^2 w}{\partial z^2} + (\alpha-1)\frac{1}{r}\frac{\partial^2}{\partial r \partial z}(ru) + F_z = \ddot{w}, \end{aligned} \tag{5.2}$$

with the traction-free boundary conditions, $\sigma_{zz} = \tau_{rz} = 0$, on the two plate surfaces, which can be written as

$$\begin{aligned} &\alpha w_{,z} + (\alpha-2)(\tfrac{u}{r} + u_{,r}) = 0 \\ &u_{,z} + w_{,r} = 0 \end{aligned} \quad \text{at } z = \pm 1. \tag{5.3}$$

The solution of Eq. (5.2) is the sum of a particular solution and the general solution of the associated homogeneous equation. The two solutions will be discussed separately.

(A) $\boldsymbol{F} \equiv [F_r, F_z]^T = \boldsymbol{0}$

To investigate the axisymmetric wave propagation in the plate without body forces, we introduce the Fourier transform with respect to t and the Hankel transform with respect to r defined by

$$\begin{aligned} \hat{\tilde{u}}(k,z,\omega) &= \int_{-\infty}^{\infty} \mathrm{e}^{-\mathrm{i}\omega t}\,\mathrm{d}t \int_0^\infty r J_1(kr) u(r,z,t)\,\mathrm{d}r, \\ \hat{\tilde{w}}(k,z,\omega) &= \int_{-\infty}^{\infty} \mathrm{e}^{-\mathrm{i}\omega t}\,\mathrm{d}t \int_0^\infty r J_0(kr) w(r,z,t)\,\mathrm{d}r, \end{aligned} \tag{5.4}$$

where $\tilde{u}, \hat{u}, \hat{\tilde{u}}, \ldots$ are the Hankel transform, Fourier transform, and the joint Hankel and Fourier transform of function u, respectively, ... Then Eqs. (5.2) and (5.3) reduce to the following ordinary differentia equations

$$\begin{aligned} &\frac{\mathrm{d}^2\hat{\tilde{u}}}{\mathrm{d}z^2} + (\omega^2 - \alpha k^2)\hat{\tilde{u}} - (\alpha - 1)k\frac{\mathrm{d}\hat{\tilde{w}}}{\mathrm{d}z} = 0, \\ &\alpha\frac{\mathrm{d}^2\hat{\tilde{w}}}{\mathrm{d}z^2} + (\omega^2 - k^2)\hat{\tilde{w}} + (\alpha - 1)k\frac{\mathrm{d}\hat{\tilde{u}}}{\mathrm{d}z} = 0 \end{aligned} \tag{5.5}$$

with

$$\begin{aligned} &\alpha\frac{\mathrm{d}\hat{\tilde{w}}}{\mathrm{d}z} + (\alpha - 2)k\hat{\tilde{u}} = 0 \\ &\frac{\mathrm{d}\hat{\tilde{u}}}{\mathrm{d}z} - k\hat{\tilde{w}} = 0 \end{aligned} \qquad \text{at } z = \pm 1. \tag{5.6}$$

Eq. (5.5) yields

$$\begin{aligned} \hat{\tilde{u}} &= a_1\cos pz + a_2\sin pz + a_3\cos qz + a_4\sin qz, \\ \hat{\tilde{w}} &= \frac{p}{k}(-a_2\cos pz + a_1\sin pz) + \frac{k}{q}(a_4\cos qz - a_3\sin qz), \end{aligned} \tag{5.7}$$

where a_i are constants to be determined, and

$$p^2 = \frac{\omega^2}{\alpha} - k^2, \qquad q^2 = \omega^2 - k^2.$$

Substituting Eq. (5.7) into the boundary conditions, Eq. (5.6), two uncoupled systems of linear equations are formed:

$$\begin{bmatrix} \dfrac{\omega^2 - 2k^2}{k}\cos p & -2k\cos q \\ -2p\sin p & -\dfrac{\omega^2 - 2k^2}{q}\sin q \end{bmatrix} \begin{Bmatrix} a_1 \\ a_3 \end{Bmatrix} = 0, \tag{5.8}$$

$$\begin{bmatrix} \dfrac{\omega^2 - 2k^2}{k}\sin p & -2k\sin q \\ 2p\cos p & \dfrac{\omega^2 - 2k^2}{q}\cos q \end{bmatrix} \begin{Bmatrix} a_2 \\ a_4 \end{Bmatrix} = 0. \tag{5.9}$$

The requirement of the nontrivial solutions for a_j leads to dispersion relation by solving the following transcendental equations:

Symmetric mode

$$(q^2 - k^2)^2\cos p\sin q + 4k^2pq\sin p\cos q = 0,$$

Antisymmetric mode

$$(q^2 - k^2)^2\sin p\cos q + 4k^2pq\cos p\sin q = 0.$$

The above two equations can be combined into one equation:

$$\omega^4 = 4k^2q^2\left[1 - \frac{p\tan(p + \gamma)}{q\tan(q + \gamma)}\right], \tag{5.10}$$

where $\gamma = 0$ and $\pi/2$ represent symmetric modes and antisymmetric modes, respectively. Eq. (5.10) is identical to the Rayleigh–Lamb equation which was derived from 2-D plane strain deformation of elastic plates. The dispersion relation results in an infinite number of wave modes ordered by $S_0, S_1, S_2, \ldots, A_0, A_1, A_2, \ldots$ for symmetric and antisymmetric modes, respectively. Figs. 1(b) and 2(b) show the first five modes S_i and A_i ($i = 1, 2, \ldots, 5$), respectively.

Based on the above analyses, we may conclude that $(\hat{\tilde{u}}, \hat{\tilde{w}})$ permit the following elementary eigensolutions of characteristic equations

$$\hat{\tilde{u}} = u_n(k, z), \quad \hat{\tilde{w}} = w_n(k, z), \quad n = 1, 2, 3, \ldots, \tag{5.11}$$

for any real k and any mode $\omega_n(k)$, where the subscript n denotes the wave modes, both symmetric and antisymmetric modes (for example, $n = 1, 3, 5, \ldots$ represent the antisymmetric modes, $n = 2, 4, 6, \ldots$ represent the symmetric modes), and (u_n, w_n) are given *via* Eqs. (5.8) and (5.9) by

$$\begin{aligned} u_n &= q_n[2k^2 \cos q_n \cos p_n z + (q_n^2 - k^2) \cos p_n \cos q_n z], \\ w_n &= k[2p_n q_n \cos q_n \sin p_n z - (q_n^2 - k^2) \cos p_n \sin q_n z], \end{aligned} \tag{5.12}$$

for symmetric modes, and

$$\begin{aligned} u_n &= q_n[2k^2 \sin q_n \sin p_n z + (q_n^2 - k^2) \sin p_n \sin q_n z], \\ w_n &= -k[2p_n q_n \sin q_n \cos p_n z - (q_n^2 - k^2) \sin p_n \cos q_n z], \end{aligned} \tag{5.13}$$

for antisymmetric modes.

To compose the complete solution the principle of superposition may be applied to the linear system for all values of k and all modes. Then, from Eq. (5.11), formally at least,

$$\begin{aligned} \hat{\tilde{u}}(z, k, \omega) &= \sum_{n=1}^{\infty} a_n(k, \omega) u_n(z, k), \\ \hat{\tilde{w}}(z, k, \omega) &= \sum_{n=1}^{\infty} a_n(k, \omega) w_n(z, k), \end{aligned} \tag{5.14}$$

where $a_n = a_n(k, \omega)$ may be determined from initial conditions or boundary conditions. The inverse transforms yield the solutions in the form

$$\begin{aligned} u(r, z, t) &= \sum_{n=1}^{\infty} \int_0^{\infty} k J_1(kr) A_n(t, k) u_n(k, z)\, \mathrm{d}k \equiv H_1^{-1}\{A_n u_n\}, \\ w(r, z, t) &= \sum_{n=1}^{\infty} \int_0^{\infty} k J_0(kr) A_n(t, k) w_n(k, z)\, \mathrm{d}k \equiv H_0^{-1}\{A_n w_n\}, \end{aligned} \tag{5.15}$$

where

$$A_n(t, k) = \frac{1}{2\pi} \int_{-\infty}^{\infty} a_n(k, \omega) \mathrm{e}^{\mathrm{i}\omega t} d\omega \equiv F^{-1}\{a_n(k, \omega)\},$$

and F^{-1}, H_0^{-1}, H_1^{-1} are the inverse operators of the Fourier, Hankel zero-order and first-order transforms, respectively.

Further, Eq. (5.15) can be evaluated by stationary phase approximation for large values of t. Eq. (5.15) with Eq. (3.19) also indicate that if a disturbance is produced at a point of an elastic plate, then the waves can be considered as plane waves at a great distance from the center of disturbance by expanding the Bessel's functions.

(B) $\boldsymbol{F} \equiv [F_r, F_z]^T \neq 0$

Now consider the transient wave in an infinite plate excited by the body forces. To construct the solution, the Hankel transform with respect to r and the Laplace transform with respect to t, are introduced for the following variables:

$$\tilde{\bar{u}}(k,z,\omega) = \int_0^\infty \mathrm{e}^{-st}\,\mathrm{d}t \int_0^\infty rJ_1(kr)u(r,z,t)\,\mathrm{d}r,$$
$$\tilde{\bar{w}}(k,z,\omega) = \int_0^\infty \mathrm{e}^{-st}\,\mathrm{d}t \int_0^\infty rJ_0(kr)w(r,z,t)\,\mathrm{d}r,$$
$$\tilde{\bar{F}}_r(z,s,k) = \int_0^\infty \mathrm{e}^{-st}\,\mathrm{d}t \int_0^\infty rJ_1(kr)F_r(r,z,t)\,\mathrm{d}r,$$
$$\tilde{\bar{F}}_z(z,s,k) = \int_0^\infty \mathrm{e}^{-st}\,\mathrm{d}t \int_0^\infty rJ_0(kr)F_z(r,z,t)\,\mathrm{d}r.$$

Then the transformed equations of Eqs. (5.2) and (5.3) can be written in the matrix form

$$L\tilde{\bar{\mathbf{U}}} - s^2\tilde{\bar{\mathbf{U}}} = -\tilde{\bar{\mathbf{F}}} \tag{5.16}$$

$$\begin{bmatrix} 1 & 0 \\ 0 & \alpha \end{bmatrix} D\tilde{\bar{\mathbf{U}}} + \begin{bmatrix} 0 & -k \\ (\alpha-2)k & 0 \end{bmatrix} \tilde{\bar{\mathbf{U}}} = \mathbf{0} \quad \text{at } z = \pm 1, \tag{5.17}$$

where $\tilde{\bar{\mathbf{U}}} = [\tilde{\bar{u}}, \tilde{\bar{w}}]^{\mathrm{T}}$, $\tilde{\bar{\mathbf{F}}} = [\tilde{\bar{F}}_r, \tilde{\bar{F}}_z]^{\mathrm{T}}$,

$$L = \begin{bmatrix} D^2 - \alpha k^2 & -(\alpha-1)kD \\ (\alpha-1)kD & \alpha D^2 - k^2 \end{bmatrix}, \quad D = \frac{\mathrm{d}}{\mathrm{d}z}, \quad D^2 = \frac{\mathrm{d}^2}{\mathrm{d}z^2}.$$

Introducing the substitution $s = \mathrm{i}\omega$, it can be readily proved that the elementary solutions $\mathbf{U}_n \equiv [u_n(k,z), w_n(k,z)]^{\mathrm{T}}$ provided by Eqs. (5.12) and (5.13) satisfy

$$L\mathbf{U}_n + \omega_n^2\mathbf{U}_n = \mathbf{0}, \tag{5.18}$$

$$\begin{bmatrix} 1 & 0 \\ 0 & \alpha \end{bmatrix} D\mathbf{U}_n + \begin{bmatrix} 0 & -k \\ (\alpha-2)k & 0 \end{bmatrix} \mathbf{U}_n = \mathbf{0} \quad \text{at } z = \pm 1.$$

Hence, $\mathbf{U}_n$ form a complete set of eigenfunctions of the plate, which are homogeneous solutions of Eq. (5.16), satisfy traction-free conditions at the plate surfaces, Eq. (5.17), and

$$\int_{-1}^{1} \mathbf{U}_m \cdot \mathbf{U}_n\,\mathrm{d}z = 0, \quad m \neq n,$$
$$\int_{-1}^{1} \mathbf{U}_n \cdot \mathbf{U}_n\,\mathrm{d}z = M_n(k) \neq 0.$$

The particular solution of the inhomogeneous Eq. (5.16) may be expressed in the form

$$\tilde{\bar{\mathbf{U}}}(z,s,k) = \sum_{n=1}^{\infty} q_n(s,k)\mathbf{U}_n(z,k), \tag{5.19}$$

where $q_n(s,k)$ is to be determined.

Substituting Eq. (5.19) into Eq. (5.16), pre-multiplying by $\mathbf{U}_n^{\mathrm{T}}$ and integrating with respect to z give

$$q_n(s,k) = \frac{1}{(s^2+\omega_n^2)M_n(k)} \int_{-1}^{1} \mathbf{U}_n^{\mathrm{T}}(z,k)\tilde{\bar{\mathbf{F}}}(z,s,k)\,\mathrm{d}z.$$

Thus, the inverse Laplace transform to Eq. (5.19) leads to

$$\widetilde{\mathbf{U}} = \sum_{n=1}^{\infty} \mathbf{U}_n Q_n / M_n,$$

with

$$Q_n(t,k) = \frac{1}{\omega_n(k)} \int_0^t F_n(\tau,k) \sin[\omega_n(t-\tau)]\,\mathrm{d}\tau,$$
$$F_n(t,k) = \int_{-1}^{1} \mathbf{U}_n^{\mathrm{T}}(z,k)\widetilde{\mathbf{F}}(z,t,k)\,\mathrm{d}z.$$

Finally, the inverse Hankel transform results in

$$\begin{aligned} u(r,z,t) &= \sum_{n=1}^{\infty} \int_0^{\infty} kJ_1(kr)\frac{u_n(z,k)}{M_n(k)} Q_n(t,k)\,\mathrm{d}k, \\ w(r,z,t) &= \sum_{n=1}^{\infty} \int_0^{\infty} kJ_0(kr)\frac{w_n(z,k)}{M_n(k)} Q_n(t,k)\,\mathrm{d}k. \end{aligned} \tag{5.20}$$

where M_n can be expressed as

$$M_n(k) = A^2\left[\frac{\omega^2}{\alpha} - (p^2-k^2)\frac{\sin 2p}{2p}\right] + D^2\left[\omega^2 + (q^2-k^2)\frac{\sin 2q}{2q}\right] + 4ADk\cos p\sin q,$$
$$A = 2kq\cos q,\quad D = (q^2-k^2)\cos p$$

for symmetric modes, and

$$M_n(k) = B^2\left[\frac{\omega^2}{\alpha} + (p^2-k^2)\frac{\sin 2p}{2p}\right] + C^2\left[\omega^2 - (q^2-k^2)\frac{\sin 2q}{2q}\right] - 4BCk\sin p\cos q,$$
$$B = 2kq\sin q,\quad C = (q^2-k^2)\sin p$$

for antisymmetric modes. For brevity the subscript n is dropped in the above equations.

Note that a set of eigenfunctions were used by Weaver and Pao (1982), Eringen and Suhubi (1975) as a complete set defined in the volume of a finite plate. The transient wave solutions in an infinite plate were constructed from that in a finite plate.

Considering a transverse point force with magnitude P at $(0,0,z_0)$, its dimensionless expression being

$$F_r = 0,\quad F_z(r,z,t) = I\frac{\delta(r)}{2\pi r}\delta(z-z_0)f(t), \tag{5.21}$$

where $I = 4P/(Gh^2)$ is the normalized magnitude of the applied force. In this case the Eq. (5.20) becomes

$$\begin{Bmatrix} u \\ w \end{Bmatrix} = \sum_{n=1}^{\infty} \int_0^{\infty} k \begin{Bmatrix} J_1(kr)u_n(z,k) \\ J_0(kr)w_n(z,k) \end{Bmatrix} \frac{w_n(z_0,k)}{M_n(k)\omega_n} h_n(t,k)\,\mathrm{d}k \tag{5.22}$$

with

$$h_n(t,k) = \frac{I}{2\pi\omega_n}\int_0^t f(\xi)\sin\omega_n(t-\xi)\,\mathrm{d}\xi,\quad n = 1,2,3,\ldots$$

If $f(t) = \delta(t)$, then

$$\begin{Bmatrix} u \\ w \end{Bmatrix} = \frac{I}{2\pi}\sum_{n=1}^{\infty} \int_0^{\infty} k \begin{Bmatrix} J_1(kr)u_n(z,k) \\ J_0(kr)w_n(z,k) \end{Bmatrix} \frac{w_n(z_0,k)}{M_n(k)\omega_n} \sin\omega_n t\,\mathrm{d}k. \tag{5.23}$$

Note that if the force P is located on the mid-plane ($z_0 = 0$), or two equal forces $P/2$ with same direction act along the z axis on the two plate surfaces at the same time, then the contribution from the symmetrical modes is zero. On the other hand, if two equal opposite forces $P/2$ act along the z axis on the two plate surfaces at the same time, then the contribution from the antisymmetric modes is zero.

If the pure impulse load is located at $\mathbf{r}' = (r', \theta', z')$ and applied at $t = t'$, the solution, which is called the Green's function for the transverse load, can be obtained by Eq. (5.23) and the coordinate transformation of displacements.

Eq. (5.23) provides the 3-D elasticity solution for the pure impulse load. For the large values of r and t, the asymptotic expansions of Eq. (5.23) is

$$u(r,z,t) \sim \frac{I}{2\pi\sqrt{rt}} \mathrm{Re} \sum_{n=1}^{\infty} \frac{k^{3/2} u_n(z,k) w_n(z_0,k)}{\sqrt{|\omega_n''|} M_n(k) \omega_n} \exp \mathrm{i}(kr - \omega_n t + \theta_1), \tag{5.24}$$

$$w(r,z,t) \sim \frac{I}{2\pi\sqrt{rt}} \mathrm{Re} \sum_{n=1}^{\infty} \frac{k^{3/2} w_n(z,k) w_n(z_0,k)}{\sqrt{|\omega_n''|} M_n(k) \omega_n} \exp \mathrm{i}(kr - \omega_n t + \theta_2), \tag{5.25}$$

where

$$\theta_1 = -\pi(\operatorname{sgn}\omega'' + 1)/4, \quad \theta_2 = -\pi(\operatorname{sgn}\omega'' - 1)/4,$$

and $k = k(r,t)$ is the stationary point which is root of the equations

$$\omega_n'(k) = \frac{r}{t}, \quad k > 0, \ \frac{r}{t} > 0.$$

Eqs. (5.24) and (5.25) become invalid if ω_n'' approaches zero. In this case the Airy approximation may be required.

Consider a radial, concentrated line force t_r (per unit length) act on $r = a$, $z = 1$ (circle on the plate top surface). If a thin circular-patch piezoelectric actuator with radius a bonded perfectly on the isotropic plate, and a time-dependent voltage is applied to the actuator, then the force applied by the actuator on the plate may be modeled by the line force.

In this case the body force $F_z = 0$, and F_r may be expressed as

$$F_r(r,z,t) = Q\delta(r-a)\delta(z-1)f(t), \tag{5.26}$$

where $Q = t_r/(Gh/2)$ is the normalized magnitude of the applied line force.

From Eq. (5.20),

$$\begin{Bmatrix} u \\ w \end{Bmatrix} = Qa \sum_{n=1}^{\infty} \int_0^{\infty} k \begin{Bmatrix} J_1(kr) u_n(z,k) \\ J_0(kr) w_n(z,k) \end{Bmatrix} J_1(ka) u_n(1,k) \frac{h_n^0(t,k)}{M_n(k)} \, \mathrm{d}k, \tag{5.27}$$

with $h_n^0(t,k) = \frac{1}{\omega_n} \int_0^t f(\tau) \sin \omega_n(t-\tau) \, \mathrm{d}\tau$.

5.1. Comparison of wave modes between plate theory and 3-D elasticity theory

The dispersion relations provided by the plate theory and 3-D elasticity theory for axisymmetric deformation can be compared. Using the same nondimensionalization which is employed in 3-D elasticity theory, the results are given below:

5.2. Symmetric mode

There is no cut-off frequency for the fundamental S_0 mode. As $k \to 0$ $c, C \sim c_P$. This limit is the same as that in the T_0 mode provided by the second-order plate theory. The S_1 and S_2 modes have cut-off frequencies $\omega_c = \pi\sqrt{\alpha}/2$ and π respectively; while the T_0 and T_1 modes give the same values of cut-off frequencies. When $k \to \infty$, the group velocities of S_0 mode approach c_R being the velocity of Rayleigh waves, all the higher modes approach the limit c_T; while $C \sim \pi/\sqrt{15}$ for T_0 mode and $C \sim c_L$ for T_1 and T_2 modes.

In Fig. 1(b), group velocity dispersion curves of three wave modes (T_0, T_1, T_2) of the plate theory and the first five wave modes $(S_0, S_1, \ldots, S_4)$ of 3-D elasticity theory for $v = 0.33$ are plotted for comparison. The fundamental T_0 and S_0 modes have a similar trend. It is worth of noting that according to the classical plate theory the T_0 mode is nondispersive. The first-order plate theory proposed by Kane and Mindlin (1956) adds the linear term in the transverse displacement w, the mode T_0 becomes dispersive, improved substantially from classical plate theory. However, the deviation of dispersive T_0 curve from the exact 3-D S_0 curve increases as ω increases. The current second-order plate theory provides a better agreement between the T_0 mode and the S_0 mode. The first fundamental T_0 dispersion curve matches well with the S_0 curve in the frequency region less than $\pi/2$ and then the group velocities of the plate theory are underestimated prior to the first cut-off frequency.

For small values of k, frequency ω decreases with increase of k for S_1 mode, thus C is negative. T_1 mode has a similar feature. The T_1 mode is close to S_1 mode in the immediate neighborhood of the cut-off frequency. Beyond the cut-off frequency, group velocities from the plate theory become overestimated for the rest of frequency region. The group velocities of both T_1 and T_2 modes from plate theory diverge from those in the S_1 and S_2 modes obtained from the exact 3-D elasticity theory when the frequency increases. From above, it shows that the second-order plate theory can better describe the extensional wave behavior in plates from low to relatively high frequency ranges than the first-order theory.

5.3. Antisymmetric mode

There is no cut-off frequency for the fundamental A_0 mode. As $k \to 0$, $\omega \sim 2\sqrt{(1-\alpha^{-1})/3}k^2$. The cut-off frequency of the A_1 mode gives $\omega_c = \pi/2$. As $k \to 0$, the higher-order plate theory leads to $\omega \sim k^2\sqrt{\alpha/3}$ for B_0 mode, $\omega_c = \pi/2$ for B_1 mode. At the high-frequency region, $C \sim c_R$ for A_0 mode, $C \sim 1$ (being normalized by c_T) for all the higher order modes A_i $(i \geqslant 1)$, but $C \sim \pi/\sqrt{12}$ and c_L for B_0 mode and B_1 mode respectively. In Fig. 2(b), group velocity dispersion curves of two wave modes (B_0, B_1) of the plate theory and the first five wave modes $(A_0, A_1, \ldots, A_4)$ of 3-D elasticity theory for $v = 0.33$ are plotted for comparison. There is a good agreement in the fundamental B_0 mode in all the frequency ranges and in the beginning part of B_1 mode. It can be seen in detail that the fundamental B_0 dispersive curve matches well with the A_0 curve in the frequency prior to $\pi/5$ and then the group velocities from the plate theory are lower than those obtained from 3-D elasticity theory. The group velocities of B_1 mode from plate theory diverge from the exact theory as the frequency increases.

6. Numerical results and discussion

Consider a plate of homogeneous, isotropic, linearly elastic material. A vertical point force is applied on the top surface of plate at $t > 0$. In this case, the wave motion in the plate is axially symmetric. The load can be expressed as body force in the form

$$\mathbf{F}(r, z, t) = I\frac{\delta(r)}{2\pi r}\delta(z - z_0)f(t)\mathbf{i}_z, \tag{6.1}$$

where $\mathbf{i}_z$ is the unit vector in the z-direction, $z_0 = 1$. Two types of transverse load are considered:

(a) seven-peak narrow-band load

$$f(t) = \left[H(t) - H\left(t - \frac{2\pi N}{p}\right)\right]\left(1 - \cos\frac{pt}{N}\right)\sin pt \quad (N = 7),$$

(b) unlimited-band pure impulse point load, $f(t) = \delta(t)$.

For the load of seven-peak signal in which a sinusoidal toneburst is modulated by a Hanning window to limit the bandwidth, two central frequencies, $p = \pi/5$, $\pi/2$, are taken in the calculation. Note that the first cut-off frequency is $\pi/2$. The value $I = 1$ is used in all cases, for convenience.

According to the higher-order plate theory, the dynamic response of the plate is sought as the superposition of responses due to the extensional load m, and the bending load q. Similarly, the wave solution of 3-D elasticity can be expressed as a summation over the symmetric and the antisymmetric modes. Both solutions based on the plate theory and based on the 3-D elasticity are presented in Figs. 3–5. Three quantities, radial displacement, u, transverse displacement, w, and the sum of in-plane strains, $\varepsilon_{\alpha\alpha} \equiv \varepsilon_r + \varepsilon_\theta$, on the top surface $z = 1$ at

$r = 300$ for the 7-peak load with $p = \pi/5$,

$r = 200$ for the 7-peak load with $p = \pi/2$,

$r = 100$ for $f(t) = \delta(t)$,

are shown in Figs. 3–5, respectively.

The solutions Eq. (3.13) and (4.17) given by the plate theory, and the solution Eq. (5.22) given by 3-D elasticity are the integral representations with the infinite upper limit $k = \infty$. They can be integrated numerically. Integration is carried in the wave number domain using trapezoidal rule, and different step sizes are applied to different regions of k. For each mode, the upper limit $k = \infty$ of the integration is replaced by a largest wave number corresponding a group velocity C which is greater than 99.5% of its limit as $k \to \infty$, and the interval of the wave number is limited by the condition $\Delta k \leqslant [3(c_L T + r)]^{-1}$, where r is the source-receiver distance, and the time duration is limited by $t < T$ (Santosa and Pao, 1989).

For the seven-peak load with $p = \pi/5$, the numerical data are evaluated from the first four modes, B_0, B_1, T_0, and T_1 of the plate theory, A_0, A_1, S_0, and S_1 modes of 3-D elasticity. In fact, the first two modes, B_0 and T_0, A_0 and S_0, are the leading terms, and the contribution from other higher-order modes may be disregarded.

For the seven-peak load with $p = \pi/2$, the plate solution includes all five modes (three extensional modes and two flexural modes), and the solution of 3-D elasticity theory is composed of the first six modes, A_i, S_i, $(i = 0, 1, 2)$. Actually, the first three modes, B_0, B_1, and T_0, A_0, A_1, and S_0 play a dominant role in the two solutions respectively, and the contribution from rest of the modes may be neglected.

Due to dispersion two wave packets can be seen in Figs. 3 and 4. The wave packet with large amplitude and low speed is dominated by A_0, or B_0 mode, and the wave packet with small amplitude and high speed is mainly caused by S_0, or T_0 mode. The effect of the higher-order modes on the entire response of the plate increases with the central frequency p.

For the pure impulse point load without the band limit, the summation over the modes is truncated at the first 10 modes, A_i, S_i, $(i = 0, 1, 2, 3, 4)$ in the 3-D elasticity solution, while all the plate wave modes are included in the solution of plate theory. Both results demonstrate a sharp disturbance with large amplitude in a short period as shown in Fig. 5, and the values of amplitude is beyond the scale of the figures. As expected, the high-frequency oscillations are not present in the higher-order plate theory.

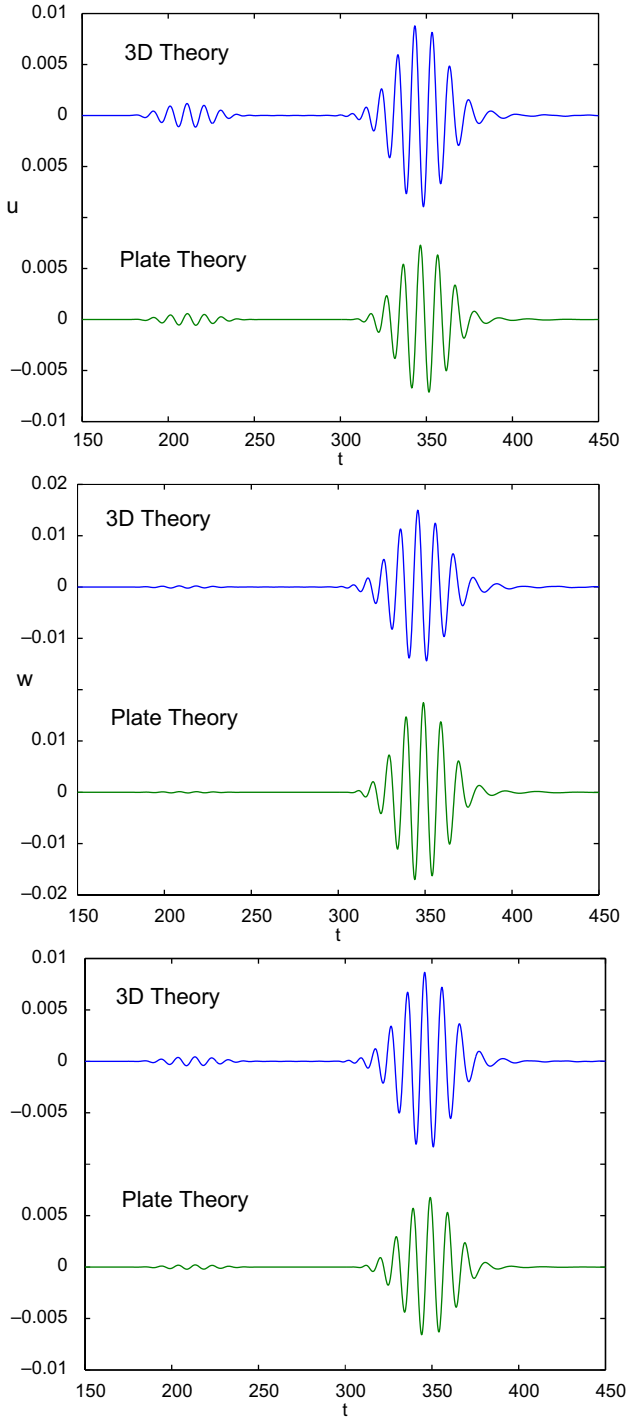

Fig. 3. The wave response, u, w, and ε_{zz}, on the top surface as a function of t under a seven-peak excitation wave ($p = 0.2\pi$) at $r = 300$.

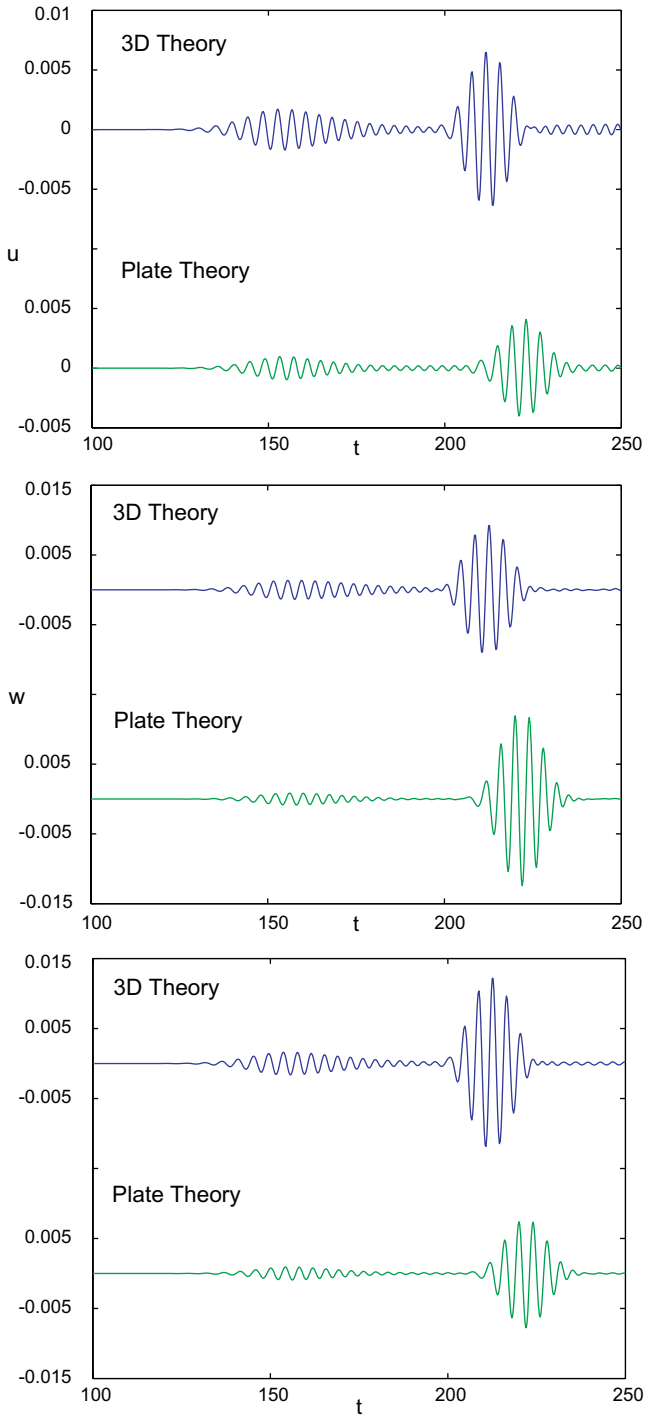

Fig. 4. The wave response, u, w, and $\varepsilon_{\alpha\alpha}$, on the top surface as a function of t under a seven-peak excitation wave ($p = \pi/2$) at $r = 200$.

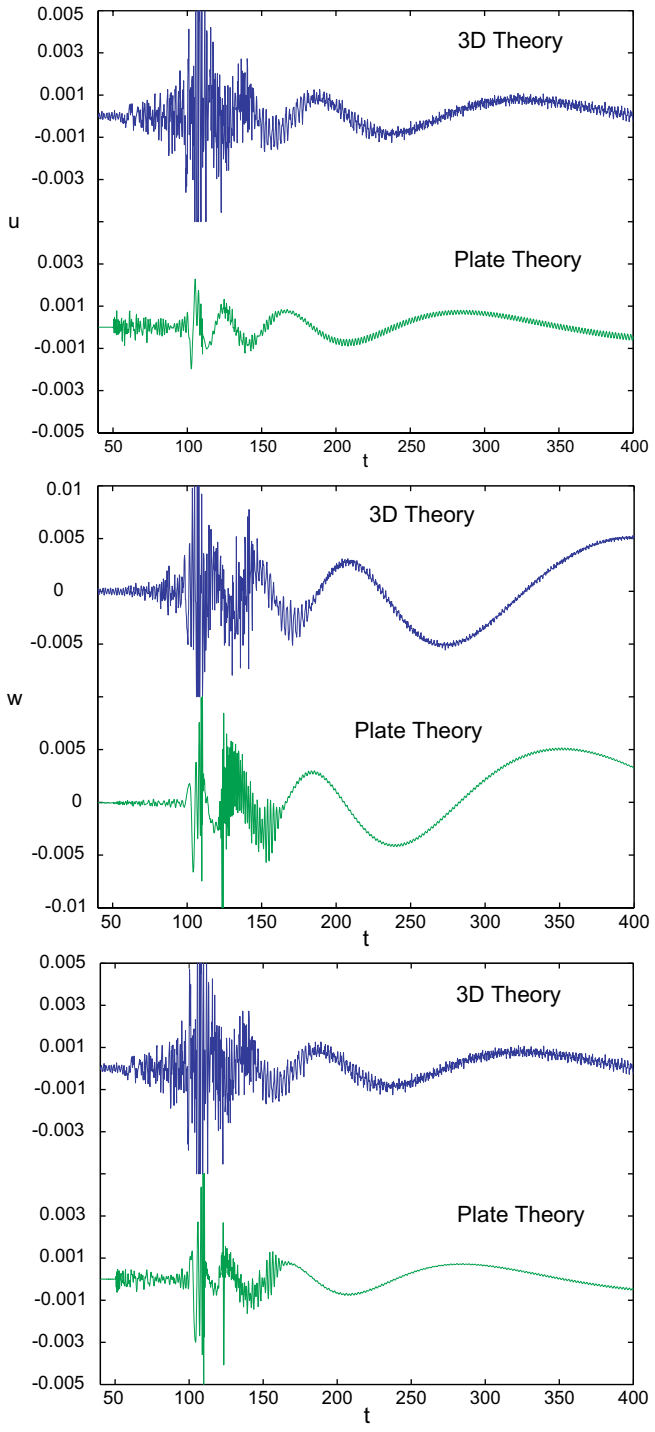

Fig. 5. The wave response, u, w, and ε_{zz}, on the top surface as a function of t under an impulse excitation wave, $f(t) = \delta(t)$, at $r = 100$.

Comparing the plate solution with the response based on 3-D elasticity shows that when the central frequency p is in the low-frequency region, the two solutions are very close to each other. Even at $p = \pi/2$ being in the middle-frequency region, the plate theory solutions can still provide fairly good results. However, the difference between the two solutions increases with p. At this central frequency $p = \pi/2 = \omega_c$, $h/\lambda_c \approx 0.6$ (λ_c is the wavelength of the first flexural mode A_0, or B_0, at $\omega = \omega_c$). Note that the classical plate theory is limited to the plates with thickness $h/\lambda_c < 0.095$ (or $h/\lambda_s < 20$ given by Junger and Feit, 1972). It seems that the validity of the plate theory is limited to the frequency range $p \leqslant \omega_c$ for a plate with $v = 0.33$.

Within the resolution of the numerical data, both solutions for the pure impulse point load exhibit a very similar pattern with some degree of phase shift, although the plate theory is incapable of modeling high-frequency response, yet this response being characterized by smaller values of amplitude. It seems that the fundamental A_0 mode makes a great contribution for the transverse load without limited band. Because the B_0 mode matches well with the A_0 mode, thus a resembling shape can be expected in the wave packets. Expanding the displacement field in its Taylor series of about $z = 0$, and retaining up first two terms for w, first three terms for u and v, the plate theory can describe the wave propagation very well at low frequencies, and provides fairly good result beyond the low-frequency region. However, at high frequency, the real displacement field can not be well characterized by its two-term, or three-term Taylor series expansion, from the view of the 3-D elasticity. Therefore, it seems that the plate solutions underestimate the amplitude of the displacement on the plate surface in the period of the sharp oscillation.

7. Conclusions

To correctly describe the wave behavior in the relatively high frequencies, a higher-order plate theory for modeling both extensional and flexural waves is developed. The aim of developing this plate theory is to provide a simple, yet accurate approach to predict the wave response in the higher frequencies range so that the smaller size of damage can be detected with good resolution used in the ultrasonic inspection techniques and structural health monitoring. The dispersion curves from the plate theory has been examined in detail and compared with those obtained from the 3-D elasticity theory. The higher-order plate theory only requires few terms to determine the wave behavior of linearly isotropic plates, thus a more efficient approach. Through integral transforms and dispersion relations, integral solutions with closed-form for a number of excitation loads based on higher-order plate theory and 3-D elasticity are developed. Green's functions are also provided. Through comparison of the wave responses based on the two theories to narrow-band seven-peak and unlimited-band pure impulse transverse loads, it can be concluded that for the narrow-banded excitation the range of validity of using higher-order plate theory is suitably applied to higher frequency ranges up to the first cut-off frequency; for unlimited band-excitation the higher-order plate theory provides reasonably similar wave packets.

Acknowledgement

This research is supported by the National Science Foundation under grants Division of Civil and Mechanical Systems (Drs. S.C. Liu and S. McCabe, Program Manager).

Appendix A. Axisymmetric wave solutions using classical plate theory

A.1. Extensional wave

A state of generalized plane stress is assumed in the linear classical plate theory. Note that the validity of classical plate theory is limited to plates where the plate thickness is less than one-twentieth of a typical

shear wavelength (Junger and Feit, 1972). According to Eq. (1.9), the dimensionless equation of motion in terms of displacement for axisymmetric extensional wave in the classical plate theory is

$$\beta\left(\nabla^2 - \frac{1}{r^2}\right)u + R = \ddot{u}, \quad t > 0, \tag{A.1}$$

where $\beta = 2/(1-\nu) = c_p^2/c_T^2$, $u = u(r,t)$ and $R = R(r,t)$ are the normalized displacement and body force in the radial direction, respectively. This equation can be solved using the joint Laplace and Hankel transforms. Applying the transforms to Eq. (A.1) and assuming zero initial conditions, the transformed solution yields

$$\tilde{\tilde{u}}(k,s) = \frac{\tilde{\tilde{R}}(k,s)}{s^2 + W^2}, \tag{A.2}$$

where $W^2 \equiv \omega^2 = \beta k^2$ is the relation between frequency ω and wave number k,

$$\begin{aligned} \tilde{\tilde{u}}(k,s) &= \int_0^\infty \exp(-st)\,\mathrm{d}t \int_0^\infty rJ_1(kr)u(r,t)\,\mathrm{d}r, \\ \tilde{\tilde{R}}(k,s) &= \int_0^\infty \exp(-st)\,\mathrm{d}t \int_0^\infty rJ_1(kr)R(r,t)\,\mathrm{d}r. \end{aligned} \tag{A.3}$$

Clearly the extensional wave based on the classical plate theory is not dispersive. Assuming the load R is a separation-of-variables type in r and t, $R(r,t) = R_r(r)f(t)$, the joint inverse transform gives the formal solution

$$u(r,t) = \int_0^\infty \frac{kJ_1(kr)}{W}\tilde{\tilde{R}}_r(k)\,\mathrm{d}k \int_0^t f(\xi)\sin W(t-\xi)\,\mathrm{d}\xi. \tag{A.4}$$

As an example of application of the solution (A.4), let the plate be compressed by two equal and opposite point forces P acting along the z axis on two surfaces of the plate. Imagine that a small cylindrical region of small radius which is separated from the plate is acted upon by the loads P, the radial reactions along the lateral boundary induced by P. From equilibrium, the uniform pressure p acting on the cylindrical surface of the plate with a small hole can be obtained ($p = 2\nu P/[(1+\nu)\pi b^2]$, b is the radius of the hole; Timoshenko and Woinowsky-Krieger, 1959). As the radius of the hole approaches zero, the radial body force for the plate with the hole can be expressed as

$$R = \frac{\nu}{\pi(1+\nu)}\frac{P}{Ghr_g}\frac{\delta(r)}{r^2}f(t) = \frac{\beta-2}{2\pi(\beta-1)}\frac{P}{Ghr_g}\frac{\delta(r)}{r^2}f(t).$$

If $f(t) = \delta(t)$, then

$$u(r,t) = \frac{I}{4\pi}\frac{\beta-2}{\beta-1}\int_0^\infty \frac{k^2}{W}J_1(kr)\sin Wt\,\mathrm{d}k, \tag{A.5}$$

$$u(r,t) \sim \frac{I}{2\pi\sqrt{2\pi\beta r}}\frac{\beta-2}{\beta-1}\int_0^\infty \sqrt{k}\sin\left(kr - \frac{\pi}{4}\right)\sin(\sqrt{\beta}kt)\,\mathrm{d}k, \text{ as } r \to \infty, \tag{A.6}$$

where $I = P/(Ghr_g)$. the horizontal load along the radial direction.

A.2. Flexural wave

According to the classical plate theory, the nondimensional equation of motion in terms displacement may and take the form

$$\ddot{w} + \alpha\nabla^2\nabla^2 w = q, \quad t > 0. \tag{A.7}$$

Applying the Laplace and the zero-order Hankel transform to Eq. (A.7) with zero initial conditions, we have

$$\tilde{\bar{w}} = \frac{\tilde{\bar{q}}}{s^2 + \alpha k^4} = \frac{\tilde{\bar{q}}}{s^2 + W^2}, \tag{A.8}$$

where $W^2 \equiv \omega^2 = \alpha k^4$, this is the dispersion relation for classical plate theory, here W represents the frequency ω, and k, the Hankel transform variable, represents the wave number. The phase and group velocities can be easily obtained as $C = 2c = \sqrt{\alpha}k$.

The inverse Laplace transform to Eq. (A.8) gives

$$\tilde{w}(k,t) = L^{-1}\left\{\frac{\tilde{\bar{q}}(k,s)}{s^2 + W^2}\right\} = \frac{1}{W}\int_0^t \tilde{q}(k,\xi)\sin W(t-\xi)\,\mathrm{d}\xi. \tag{A.9}$$

For the point load, $q = \frac{1}{2\pi}\frac{\delta(r)}{r}f(t)$, Eq. (A.9) becomes

$$\tilde{w}(k,t) = \frac{1}{2\pi W}\int_0^t f(\xi)\sin W(t-\xi)\,\mathrm{d}\xi. \tag{A.10}$$

If the point load is the rectangular impulse, $f(t) = [H(t) - H(t-T)]q_0$, Eq. (A.9) becomes

$$\tilde{w}(k,t) = \frac{q_0}{2\pi}\frac{(1-\cos Wt)}{W^2} \quad \text{for } 0 < t < T, \tag{A.11}$$

$$\tilde{w}(k,t) = \frac{q_0}{2\pi}\frac{\cos W(t-T) - \cos Wt}{W^2} \quad \text{for } T < t. \tag{A.12}$$

By the Hankel inverse transform,

$$w(r,t) = \frac{q_0}{2\pi}\int_0^\infty kJ_0(kr)\frac{(1-\cos Wt)}{W^2}\,\mathrm{d}k \quad \text{for } 0 < t < T, \tag{A.13}$$

$$w(r,t) = \frac{q_0}{2\pi}\int_0^\infty kJ_0(kr)\frac{\cos W(t-T) - \cos Wt}{W^2}\,\mathrm{d}k \quad \text{for } T < t. \tag{A.14}$$

Sneddon (1951) and Medick (1961) defined a function

$$F(x) = \pi/2 - Si(x) - xCi(x) - \sin x, \tag{A.15}$$

where $Si(x)$ and $Ci(x)$ are the sine and cosine integrals. Then the following integral can be expressed as

$$\int_0^\infty J_0(\xi)\frac{1-\cos\beta\xi^2}{\xi^3}\,\mathrm{d}\xi = \frac{1}{2}F\left(\frac{1}{4\beta}\right). \tag{A.16}$$

Using Eq. (A.16) and replacing kr by ξ, Eqs. (A.13) and (A.14) may be written as

$$w(r,t) = \frac{q_0 t}{4\pi\sqrt{\alpha}}F\left(\frac{r^2}{4\sqrt{\alpha}t}\right), \quad 0 < t < T, \tag{A.17}$$

$$w(r,t)=\frac{q_0}{4\pi\sqrt{\alpha}}\left\{tF\left(\frac{r^2}{4\sqrt{\alpha}t}\right)-(t-T)F\left[\frac{r^2}{4\sqrt{\alpha}(t-T)}\right]\right\},\quad t>T. \tag{A.18}$$

This solution is called Medick solution. For large values of r and t, the solution for classical plate theory approaches asymptotically

$$w(r,t)\sim\frac{8\sqrt{\alpha}q_0}{\pi\sqrt{rt}}\left(\frac{r}{t}\right)^{-7/2}\sin\left[\frac{T}{8\sqrt{\alpha}}\left(\frac{r}{t}\right)^2\right]\mathrm{Re}\left\{\exp\left[i\frac{T}{8\sqrt{\alpha}}\left(\frac{r}{t}\right)^2\right]e^{i\frac{r/t}{2\sqrt{\alpha}}(r-0.5\frac{r}{t}t)}\right\} \tag{A.19}$$

or

$$w(r,t)\sim\frac{q_0T}{\pi\sqrt{rt}}\left(\frac{r}{t}\right)^{-3/2}\cos\left[\frac{1}{2\sqrt{\alpha}}\frac{r}{t}\left(r-\frac{1}{2}\frac{r}{t}t\right)\right],\quad T\ll 1\ll t. \tag{A.20}$$

If $f(t)=\delta(t)$, since

$$\delta(t)=\frac{\mathrm{d}H(t)}{\mathrm{d}t}=\frac{H(t)-H(t-T)}{T},\quad \text{as } T\to 0,$$

from (A.10) and (A.18),

$$w(r,t)=\frac{q_0}{2\pi}\int_0^\infty kJ_0(kr)\frac{\sin Wt}{W}\,\mathrm{d}k=\frac{q_0}{4\pi\sqrt{\alpha}}\left[F\left(\frac{r^2}{4\sqrt{\alpha}t}\right)-\frac{r^2}{4\sqrt{\alpha}t}F'\left(\frac{r^2}{4\sqrt{\alpha}t}\right)\right].$$

Note the asymptotic expansion, Eq. (A.20), is identical to that for the pure impulse, $q=\frac{q_0T}{2\pi}\frac{\delta(r)}{r}\delta(t)$. If Eq. (A.19), or (A.20), is to be written in a form as $w\sim\mathrm{Re}\{A(r,t)e^{i\theta(r,t)}\}$, it is ready to show a flexural wavetrain with phase velocity $c=0.5r/t$, the wave amplitude decreases like $(r/t)^{-1/2}$ along a ray $r/t=C$, and $|A|^2$, or the energy, propagates with the group velocity $C=r/t$.

References

Achenbach, J.D., 1984. Wave Propagation in Elastic Solids. North-Holland Publishing Company, Amsterdam.

Alleyne, D.N., Cawley, P., 1992. Optimization of lame wave inspection technique. NDT & E International 25, 11–22.

Bray, D.E., McBride, D., 1992. Nondestructive Testing Techniques. John Wiley & Sons, Inc., New York.

Cawley, P., Alleyne, D.N., 1996. The use of lamb waves for the long range inspection of large structures. Ultrasonics 34, 287–290.

Debnath, L., 1995. Integral Transforms and Their Applications. CRC Press Inc., Boca Raton, FL.

Eringen, A.C., Suhubi, E.S., 1975Elastodynamics Linear Theory, vol. 2. Academic Press, New York.

Graff, K.F., 1991. Wave Motion in Elastic Solids. Dover Publications, New York.

Jeffreys, H., Jefferys, B.S., 1956. Methods of Mathematical Physics, third ed. Cambridge Press.

Junger, M.C., Feit, F., 1972. Sound, Structures, and Their Interaction. MIT Press, Cambridge, MA.

Kane, T.R., Mindlin, R.D., 1956. High-frequency extensional vibrations of plates. ASME, Journal of Applied Mechanics 23, 277–283.

Krautkramer, J., Krautkramer, H., 1990. Ultrasonic Testing of Materials. Springer-Verlag, Berlin.

Lih, S.S., Mal, A.K., 1995. On the accuracy of approximation plate theories for wave field calculations in composite laminates. Wave Motion 21, 17–34.

Medick, M.A., 1961. On classical plate theory and wave propagation. ASME Journal of Applied Mechanics 28, 223–228.

Mindlin, R.D., 1951. Influence of rotatory inertia and shear in flexural motions of isotropic elastic plates. ASME Journal of Applied Mechanics 18, 31–38.

Mindlin, R.D., Medick, M.A., 1959. Extensional vibrations of elastic plates. Journal of Applied Mechanics 26, 561–569.

Reissner, E., 1945. The effect of transverse shear deformation on the bending of elastic plates. ASME Journal of Applied Mechanics 12, A69–A77.

Reissner, E., 1947. On bending of elastic plates. Quarterly of Applied Mathematics 5 (1), 55–68.

Rose, J.L., 1999. Ultrasonic Waves in Solid Media. Cambridge University Press, Cambridge, UK.

Santosa, F., Pao, Y.H., 1989. Transient axially asymptotic response of an elastic plate. Wave Motion 11, 271–295.

Sneddon, I.N., 1951. Fourier Transforms. McGraw-Hill Book Company, Inc., New York.
Stamnes, J.J., 1986. Waves in Focal Regions. IOP Publishing Limited, England.
Timoshenko, S., Woinowsky-Krieger, S., 1959. Theory of Plate and Shells. McGraw-Hill, New York.
Washizu, K., 1982. Variational Methods in Elasticity and Plasticity, third ed. Pergamon Press, Oxford.
Weaver, R.L., Pao, Y.H., 1982. Axisymmetric elastic waves excited by a point source in a plate. ASME Journal of Applied Mechanics 49, 821–836.
Whitney, J.M., Sun, C.T., 1973. A higher order theory for extensional motion of laminated composites. Journal of Sound and Vibration 30 (1), 85–97.